

1 Electronic energy transfer on a vibronically coupled quantum aggregate

2 Jan Roden,^{1,a)} Georg Schulz,^{2,b)} Alexander Eisfeld,^{1,c)} and John Briggs^{1,2,d)}

3 ¹Max Planck Institute for the Physics of Complex Systems, Dresden 01187, Germany

4 ²Theoretical Quantum Dynamics, Physics Institute, University of Freiburg, Germany

5 (Received 7 May 2009; accepted 23 June 2009; published online xx xx xxxx)

AQ: 6 We examine the transfer of electronic excitation (an exciton) along a chain of electronically coupled
#1 7 monomers possessing internal vibronic structure and which also interact with degrees of freedom of
8 the surrounding environment. Using a combination of analytical and numerical methods, we
9 calculate the time evolution operator or time-dependent Green's function of the system and thereby
10 isolate the physical parameters influencing the electronic excitation transport. Quite generally, we
11 show that coupling to vibrations slows down and inhibits migration of electronic excitation due to
12 dephasing effects on the coherent transfer present without vibrations. In particular, coupling to a
13 continuous spectrum of environment states leads to a complete halting of transfer, i.e., a trapping of
14 the exciton. © 2009 American Institute of Physics. [DOI: 10.1063/1.3176513]
15

16 I. INTRODUCTION

17 The problem of the time dependence and character of
18 electronic excitation transport (EET) along aggregates of at-
19 oms, molecules, or other monomeric quantum objects is en-
20 joying renewed interest in the light of refined experimental,
21 device fabrication, and molecular manipulation techniques.
22 Apart from traditional quantum aggregates, such as those
23 composed of organic molecules, e.g., crystals,¹⁻⁴
24 dendrimers,⁵ *J*-aggregates,⁶ photosynthetic units,⁷⁻¹¹ new
25 types of aggregate, such as cold atom¹²⁻¹⁴ or quantum dot
26 assemblies,¹⁵ mixed aggregates of metal nanoparticles, and
27 organic molecules,¹⁶ are being studied. New, more sophisti-
28 cated probing and detection techniques allow studies on EET
29 with increasing spatial and temporal resolutions. In some
30 cases, the nature of EET on such aggregates is considered to
31 be due to the quantum coherence embodied in the very con-
32 cept of the delocalized exciton. This coherence is affected
33 strongly by the interaction with the “environment,” usually
34 in the form of nuclear vibrations, and hence such interac-
35 tions, leading to decoherence, alter the nature and probability
36 of migration of electronic excitation along the aggregate.

37 In this paper we will concentrate on the molecular Fren-
38 kel exciton problem, considering molecular aggregates com-
39 posed of monomers whose absorption bands show broad vi-
40 brational structure. Since the molecules in weakly bound
41 aggregates largely retain their character, we will use the lan-
42 guage of molecular rather than solid-state physics. In a mo-
43 lecular aggregate, usually studied in solution, the electronic
44 excitation interacts with various types of vibration, as classi-
45 fied in Ref. 17. First and foremost, there are the intramolecu-
46 lar vibrational excitations directly accompanying light ab-
47 sorption due to a shift of the equilibrium position of the
48 nuclei on electronic excitation. These primary intramolecular
49 vibrations we call internal modes (IMs). They are evident in

the absorption spectra of isolated monomers and usually 50
dominated by one or a few normal modes. At low tempera- 51
tures, these modes can clearly be seen.¹⁸ In large organic 52
molecules, these primary vibrations couple to many other 53
IMs so that the absorption spectrum consists of many vi- 54
bronic lines. In solution, the intramolecular vibrations inter- 55
act with a myriad of lower frequency modes (arising from 56
the increase in the mass of the vibrators) representing 57
phonons on the aggregate itself or vibrational, rotational, and 58
translational degrees of freedom of the surrounding liquid 59
molecules. We will call such external modes, specified usu- 60
ally only by a continuous mode density, EMs. In addition, 61
there is a broadening due to local variations in the electronic 62
interaction of a given monomer with the surrounding mol- 63
ecules. 64

The objective of this paper is to study the propagation of 65
an initially localized electronic excitation along a molecular 66
aggregate, interacting with both IM and EM vibrations. The 67
relevant time scales are then (a) the typical time T_{el} for trans- 68
fer of electronic excitation due to intermonomer coupling 69
and (b) the typical time T_{vib} for the onset of electronic- 70
vibrational coupling. In the energy picture these times corre- 71
spond to the half-width $B = \hbar/T_{el}$ of the exciton band and the 72
width $\sigma = \hbar/T_{vib}$ of the monomer vibronic absorption spec- 73
trum. 74

In the specific case of molecular aggregates, this EET 75
problem has been tackled using two rather distinct sets of 76
approximation to the full problem, which lead to two differ- 77
ent pictures of the transfer process. 78

(1) On the one hand, and by far the most popular approach, 79
the intramolecular vibrations are not considered explic- 80
itly and interest is centered on the influence of coupling 81
to the surroundings. This follows the methods of solid- 82
state physics and usually the language is that of second 83
quantization and linear exciton-phonon coupling. In the 84
zeroth order, an aggregate is taken to consist of mono- 85
mers with only a single sharp electronic transition line. 86
Due to coupling to the surrounding, each monomer at a 87

^{a)}Electronic mail: roden@mpipks-dresden.mpg.de.

^{b)}Electronic mail: georg.schulz@physik.uni-freiburg.de.

^{c)}Electronic mail: eisfeld@mpipks-dresden.mpg.de.

^{d)}Electronic mail: john.briggs@physik.uni-freiburg.de.

88 different site along the aggregate is subject to fluctuat-
 89 ing forces, which leads to a change in the effective
 90 electronic transition energy and/or in the strength of
 91 electronic coupling to neighboring monomers. The
 92 shifts and coupling changes are then treated statistically
 93 according to some prescription. A distinction between
 94 IM and EM is not made usually, all being treated sim-
 95 ply as phonons. Indeed, often the precise origin of
 96 monomer transition energy fluctuations, whether from
 97 changed electronic interaction with fluctuating sur-
 98 roundings, from local inhomogeneities, or from inter-
 99 action with vibrations, rotations, or translations of the en-
 100 vironment, need not be specified. Rather, those
 101 fluctuations are treated as distributions whose character
 102 can be assumed and whose effect can be described via
 103 fit parameters to explain the experimental data. This
 104 disorder model has been applied extensively in the en-
 105 ergy domain (as examples see Refs. 19–22), beginning
 106 with the works of Schreiber and Toyozawa¹⁹ and
 107 Knapp.²³ The main effect of disorder in the transition
 108 energies is to localize the otherwise delocalized purely
 109 electronic excitonic wave functions. This effect is illus-
 110 trated clearly in the works of Malyshev and co-workers.
 111 ^{24–26} When transfer in the time domain is
 112 considered in this model, the varying excitation energy
 113 barriers between monomers lead to trapping of excita-
 114 tion in these localized regions. Finite temperature may
 115 provoke a jumping over these barriers and renewed
 116 transport.^{27,28} The final picture is one of hopping be-
 117 tween these localized regions with essential destruction
 118 of coherent exciton transfer except within the limited
 119 domains of the localized wave functions.

120 (2) On the other hand, which is the approach of the present
 121 paper, one uses the molecular language of wave func-
 122 tions and Green's functions built from them. First one
 123 recognizes that all organic molecules possess rich inter-
 124 nal vibrational structure. Then one must take the in-
 125 tramolecular IM modes of identical monomers explic-
 126 itly into account. Transitions into and out of the
 127 electronically excited state as the exciton propagates
 128 are accompanied by transitions, weighed by Franck-
 129 Condon (FC) factors, into and out of vibrational states.
 130 This leads to an effective dilution of the electronic cou-
 131 pling and effective variations in the transition energies.
 132 The influence of the surroundings is then taken into
 133 account by considering their vibrational states to be
 134 continuously distributed, corresponding to coupling to
 135 an open system, and leading to a continuous absorption
 136 spectrum. Now there is essentially a continuous distri-
 137 bution of vertical transition energies and a continuous
 138 distribution of electronic monomer-monomer coupling
 139 strengths via the continuous FC factor. Hence the pic-
 140 ture of transport which emerges is much more compli-
 141 cated than that of pure electronic excitation transfer.

142 The monomer models appropriate to the method de-
 143 scribed in (2) are illustrated in the sketch of Fig. 1. We con-
 144 sider a ground-state Born–Oppenheimer (BO) potential well.
 145 When the monomer absorption spectrum exhibits some dis-

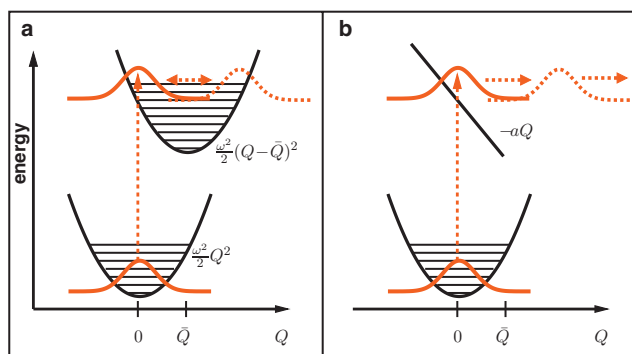


FIG. 1. Sketch of the lower and upper monomer BO potential curves: (a) with discrete levels in the upper potential (reflected wavepacket) and (b) with a continuum (outgoing wavepacket).

crete IM structure, the left figure (a) is applicable, in which
 absorption is to discrete states of the upper BO potential. A
 popular simplification is to take the ground and upper BO
 potentials to be of the same harmonic form, giving vibra-
 tional spacing $\hbar\omega$ but with the minimum of the upper po-
 tential shifted by an amount \bar{Q} from that of the ground state.
 Then the FC factors can be expressed in a closed form. For
 example, when absorption is from the lowest state of the
 ground BO potential to vibrational states α of the upper po-
 tential, one has the FC factor f_0^α with

$$|f_0^\alpha|^2 = \frac{X^\alpha}{\alpha!} \exp(-X), \quad (1)$$

i.e., a Poisson distribution of FC factors. Here X is the di-
 mensionless Huang–Rhys factor $X = \omega\bar{Q}^2/2\hbar$.²⁹ In this case
 the absorption band has width (standard deviation) $\sigma = \sqrt{X}$ in
 units of the vibrational energy quantum $\hbar\omega$.

Clearly the establishment of discrete vibronic structure
 requires multiple reflections of the wavepacket on the upper
 potential, as illustrated schematically in Fig. 1(a). Interaction
 with EM corresponds to suppression of 100% reflection at
 the outer turning point and a broadening of the vibronic line.
 The limit of continuous broadening is mimicked by effec-
 tively moving the outer turning point to infinity, giving a
 purely outgoing vibrational wavepacket. Then, in the region
 of FC overlap, the upper potential can be modeled by a linear
 potential, as sketched in Fig. 1(b). As shown in Appendixes
 A and B (see also Refs. 30 and 31), this gives rise to a single
 continuous monomer absorption peak. Also this procedure
 corresponds to taking a particular limit of the discrete spec-
 trum in Fig. 1(a). This limit is $X \rightarrow \infty, \omega \rightarrow 0$ in the upper
 electronic potential such that the spectral width $\sqrt{X}\hbar\omega$ re-
 mains constant. This will be used later in numerical work to
 represent a continuously broadened absorption spectrum.

We have applied extensively the approach described in
 (2) in the energy domain mainly to calculate aggregate ab-
 sorption spectra.^{32–37} However, the theory, which uses an
 energy-dependent Green's function approach, could also be
 used to estimate the range of propagation of excitons of
 given energy interacting with a continuous distribution of
 vibrational modes.^{32,33} The results showed a clear curtail-
 ment of exciton propagation length depending on the
 strength of the vibronic coupling compared to the electronic

AQ:
#2AQ:
#3

187 monomer-monomer coupling. Here we return to this problem
188 but treat it explicitly in the time domain by the use of the
189 time-dependent Green's function (time propagator) for the
190 vibronically coupled aggregate including both discrete IM
191 vibrations and continuous environment EM.

192 The plan of the paper is as follows. In Sec. II we define
193 the vibronic Hamiltonian of the aggregate and introduce the
194 time-dependent and time-independent Green's operators
195 (propagators) of both monomer and aggregate. The main aim
196 of the paper is to examine first the influence of IM alone on
197 EET and then to extend consideration to the additional cou-
198 pling to a broad continuum of EM. In this way we isolate the
199 effects of discrete and continuous modes. However, the ex-
200 plicit effect of energy dissipation due to coupling with the
201 surroundings and the related effect of changing temperature
202 will largely not be taken into account. That is, we will as-
203 sume that the vibrational state of an excited molecule is not
204 changed due to vibrational interaction but only due to elec-
205 tronic interaction.

206 In this paper, strong and weak couplings will be defined
207 according to the criterion introduced by Simpson and
208 Peterson³⁸ as the ratio between the exciton band half-width B
209 and the width σ of the monomer absorption spectrum. This
210 dimensionless Simpson–Peterson (SP) parameter will be
211 called $SP=B/\sigma=T_{\text{vib}}/T_{\text{el}}$. Strong coupling occurs when this
212 value is much greater than unity and weak coupling when
213 much less than unity. All other cases are designated as inter-
214 mediate coupling.

215 In Sec. III we consider an exciton on a one-dimensional
216 aggregate coupled to a single IM mode of the monomers.
217 First, the problem is treated exactly in that the full aggregate
218 vibronic Hamiltonian is represented by expansion in a suit-
219 able set of vibronic basis states, chosen large enough to en-
220 sure convergence. Then the time-dependent Schrödinger
221 equation is solved by propagation numerically in time. This
222 allows calculation of the probability $P_{n0}(t)$ that electronic
223 excitation, initially localized on monomer zero, has arrived
224 at monomer n at time t . Due to limits on computer storage,
225 the exact calculations are restricted to rather short aggre-
226 gates. However, we also calculate $P_{n0}(t)$ in the “coherent
227 exciton scattering” (CES) approximation.^{32,33} In this approxi-
228 mation, only the ground vibrational state of the ground elec-
229 tronic state is taken into account. With this limitation, calcu-
230 lations are possible for very large aggregates. In Sec. III we
231 show that the CES approximation gives generally good
232 agreement with the exact calculations. Hence in the rest of
233 the paper, the CES approximation is used.

234 The numerical solution of the time-dependent
235 Schrödinger equation is equivalent to a numerical evaluation
236 of the time-dependent propagator or Green's function. In
237 Sec. IV we show first that in both limits of strong coupling
238 and extreme weak coupling, in the CES approximation the
239 time-dependent Green's function can be evaluated analyti-
240 cally. This yields analytic forms for $P_{n0}(t)$, which are the
241 closed form expressions derived separately by Merrifield³⁹
242 and Bierman.⁴⁰ Finally in CES approximation, $P_{n0}(t)$ is
243 evaluated numerically for all coupling strengths and for large
244 aggregates, initially for monomers with only one IM discrete
245 mode of internal vibration and then for a more realistic case

where continuous EMs are also included. In this latter case 246
we use a fit to a measured continuous monomer absorption 247
spectrum of the pseudoisocyanine (PIC) dye. Inclusion of 248
coupling to EM gives rise to a qualitatively new effect, 249
namely, trapping of the exciton. In Sec. IV D an approximate 250
analytic solution, originally due to Magee and Funabashi,⁴¹ 251
is derived which allows the trapping phenomenon to be ex- 252
plained. A summary of results and our conclusions are given 253
in Sec. V. 254

II. AGGREGATE HAMILTONIAN AND GREEN'S FUNCTION 255

In this work, for simplicity, we will restrict discussion to 257
a one-dimensional aggregate consisting of N monomers. The 258
EET along the aggregate will be investigated in two ways. In 259
the numerically exact method, the aggregate state is propa- 260
gated in time by solving the time-dependent Schrödinger 261
equation 262

$$i\hbar\partial_t|\Psi(t)\rangle = H|\Psi(t)\rangle, \quad (2) \quad 263$$

with the total aggregate vibronic Hamiltonian H expressed 264
on the basis of aggregate vibronic states (taking into account 265
enough states to ensure convergence). The solution of this 266
equation is equivalent to solving for the time-dependent 267
propagator, or time-dependent Green's operator, 268

$$G(t) = \exp(-iHt/\hbar)\Theta(t). \quad (3) \quad 269$$

In the second method, useful for analytic evaluation, the 270
time-dependent Green's function, i.e., the operator $G(t)$ ex- 271
pressed in a vibronic basis, is obtained in closed form, in 272
strong and weak-coupling limits, by using the CES approxi- 273
mation to the energy-dependent Green's function, followed 274
by a Fourier transform to the time representation. 275

For very long aggregates, constraints on computer stor- 276
age oblige us to use an approximation also in the first method 277
when solving the time-dependent Schrödinger equation nu- 278
merically. The approximation we choose is equivalent to the 279
CES approximation, hence combining the two methods. 280

We adopt a model of an aggregate composed of mono- 281
mers with one excited electronic state and one vibrational 282
degree of freedom leading to a single vibrational progression 283
in monomer absorption from the ground state. The lower and 284
upper potential curves can, but do not have to, be harmonic 285
as in the standard approach. Simply we assume that the up- 286
per curve minimum is shifted from that of the ground elec- 287
tronic state to a larger distance. The nature of the vibrations 288
is then expressed solely in the discrete or continuous distri- 289
bution of FC factors describing transitions between vibra- 290
tional states of the lower and upper manifolds. The mono- 291
mers are coupled electronically and it is assumed that this 292
coupling is independent of vibrational coordinates. The 293
monomer and aggregate Hamiltonians are identical to those 294
described in detail in Refs. 32, 33, and 35, where the absorp- 295
tion spectra of J - and H -aggregates were presented. The 296
Hamiltonian and Green's operators will be expressed in 297
terms of basis states in which electronic excitation is local- 298
ized on one monomer, i.e., we define 299

$$|\pi_n\rangle := |\phi_n^e\rangle \prod_{m \neq n} |\phi_m^g\rangle, \quad (4)$$

300

301 where $|\phi_n^e\rangle$ and $|\phi_n^g\rangle$ are the ground and excited electronic
302 states of monomer n , respectively (the monomers are taken
303 to be identical). In this basis, the Green's operator has elec-
304 tronic matrix elements

$$G_{nm}(t) = \langle \pi_n | G(t) | \pi_m \rangle, \quad (5)$$

305 which are still operators in the space of nuclear coordinates.
306 If the aggregate state at time zero is denoted by $|\Psi(0)\rangle$, the
307 state at later times is given by

$$|\Psi(t)\rangle = G(t)|\Psi(0)\rangle. \quad (6)$$

310 To consider excitation propagation, we must specify the ini-
311 tial state. The simplest way to study EET is to assume that an
312 arbitrary monomer, let us call it monomer 0, alone is excited
313 at time zero. Since electronic excitation can be considered
314 instantaneous on vibrational time scales, then the appropriate
315 initial aggregate vibrational state is that with all monomers in
316 their respective vibrational ground state, i.e.,

$$|\Psi(0)\rangle = |\pi_0\rangle |\Sigma_g\rangle, \quad (7)$$

317 where

$$|\Sigma_g\rangle = \prod_m |\xi_m^0\rangle \quad (8)$$

319

320 and $|\xi_m^0\rangle$ is the lowest vibrational state of the ground elec-
321 tronic state of monomer m . The vibronic basis states where
322 one monomer is excited electronically are defined as a
323 straightforward generalization of Eqs. (4) and (8), i.e.,

$$|\pi_n\rangle |\{\alpha\}_n\rangle = |\pi_n\rangle |\xi_1^{\alpha_1} \cdots \chi_n^{\alpha_n} \cdots \xi_N^{\alpha_N}\rangle, \quad (9)$$

324 where $\chi_n^{\alpha_n}$ is the vibrational wave function of the electroni-
325 cally excited monomer n with α_n vibrational quanta and the
326 remaining α_i denotes the vibrational quanta in the ground
327 electronic state of each monomer i . Throughout the work we
328 will use χ to denote vibrational states of an electronically
329 excited monomer and ξ for the vibrational states of a mono-
330 mer in the electronic ground state.

331 The probability $P_{n0}(t)$ that the electronic excitation re-
332 sides on monomer n at time t is given by

$$P_{n0}(t) = \sum_{\{\alpha\}} |\langle \{\alpha\}_n | \langle \pi_n | \Psi(t) \rangle|^2 = \sum_{\{\alpha\}} |\langle \{\alpha\}_n | G_{n0}(t) | \Sigma_g \rangle|^2, \quad (10)$$

334

335 where a summation has been made over all possible final
336 vibrational states of the aggregate when monomer n is ex-
337 cited electronically.

338 Next, for later use, we consider energy-dependent
339 Green's operators from which the time-dependent ones can
340 be calculated by Fourier transformation. For noninteracting
341 monomers we define the energy-dependent Green's operator
342 at energy E as

$$g(E) = (E - H_{\text{mon}} + i\delta)^{-1}, \quad \delta = 0_+, \quad (11)$$

343 where H_{mon} is the total vibronic Hamiltonian of noninteract-
344 ing monomers. Denoting the electronic coupling operator be-
345 tween monomers by V , then $H = H_{\text{mon}} + V$ is the total aggre-

gate vibronic Hamiltonian and the energy-dependent 347
aggregate Green's operator is 348

$$G(E) = (E - H + i\delta)^{-1}. \quad (12) \quad 349$$

The aggregate Green's operator satisfies the equation 350

$$G(E) = g(E) + g(E)V G(E). \quad (13) \quad 351$$

To consider the propagation of electronic excitation in time, 352
we need the time-dependent Green's operators defined by 353
Eq. (3) for the full Hamiltonian and by 354

$$g(t) = \exp(-iH_{\text{mon}}t/\hbar)\Theta(t) = \frac{i}{2\pi} \int_{-\infty}^{\infty} g(E)e^{-i\hbar Et} dE \quad (14) \quad 355$$

for propagation by noninteracting monomers. 356

In the electronic basis (4), the Dyson equation (13) reads 357
as 358

$$G_{nm}(E) = g_n(E)\delta_{nm} + g_n(E) \sum_{n'} V_{nn'} G_{n'm}(E). \quad (15) \quad 359$$

Note that G_{nm} and g_n are still operators in the space of 360
nuclear coordinates. However, we will ignore the nuclear 361
coordinate dependence of the electronic coupling matrix el- 362
ements $V_{nn'}$ and take them to be constants for fixed inter- 363
monomer separation and orientation. Then, in the time do- 364
main, Eq. (15) reads as 365

$$G_{nm}(t) = g_n(t)\delta_{nm} + \int_0^{\infty} g_n(t-t') \sum_{n'} V_{nn'} G_{n'm}(t') dt'. \quad (16) \quad 366$$

Equations (10), (15), and (16) will be used in the following 367
to discuss the EET process. 368

III. NUMERICALLY EXACT TIME PROPAGATION: 369 COUPLING TO ONE DISCRETE VIBRATIONAL MODE 370

In order to solve the time-dependent Schrödinger equa- 371
tion (2) numerically, the aggregate vibronic Hamiltonian and 372
the time-dependent aggregate state $|\Psi(t)\rangle$ will be expressed 373
in a truncated set of the vibronic basis states of Eq. (9). Then 374
the time propagation is calculated straightforwardly using a 375
fourth order Runge–Kutta algorithm. The Hamiltonian ma- 376
trix elements in this basis are 377

$$\langle \{\alpha\}_n | \langle \pi_n | H | \pi_m \rangle | \{\beta\}_m \rangle \quad 378$$

$$= \epsilon^{\{\alpha\}_n} \delta_{nm} \delta_{\{\alpha\}_n \{\beta\}_m} + V_{nm} f_{\beta_n}^{\alpha_n} (f_{\alpha_n}^{\beta_n}) \prod_{i=1}^N \delta_{\alpha_i \beta_i}, \quad (17) \quad 379$$

where $\epsilon^{\{\alpha\}_n}$ is the sum of the monomer electronic excitation 380
energy ϵ_{el} of monomer n and all vibrational quanta in the 381
state $|\pi_n\rangle |\{\alpha\}_n\rangle$. The FC overlap matrix elements are defined 382
as 383

$$f_{\beta_n}^{\alpha_n} = \langle \chi^{\alpha_n} | \xi^{\beta_n} \rangle, \quad (18) \quad 384$$

denoting a transition from the state ξ^{β_n} of the lower potential 385
to the state χ^{α_n} in the upper potential curve of monomer n . 386
Then we use Eqs. (2) and (10) to calculate the time- 387

AQ:
#4AQ:
#5

TABLE I. Relations between quantities used: T_{el} is the typical time for EET, B is the half-width of the exciton band, T_{vib} is the typical time for electronic-vibrational coupling, σ is the width of the monomer vibronic absorption spectrum, SP is the Simpson–Peterson parameter, $V=V_{n,n+1}$ is the nearest-neighbor electronic intermonomer interaction, X is the Huang–Rhys parameter, ω is the vibrational frequency, and \bar{Q} is the shift of the harmonic BO potentials.

$T_{el}=\hbar/B$	$T_{vib}=\hbar/\sigma$	$SP=B/\sigma$
$B=2V$	$\sigma=\sqrt{X}\hbar\omega$	$X=\omega\bar{Q}^2/2\hbar$

dependent probability that a given monomer n is excited electronically.

The dynamics of excitation transfer depend essentially on the dimensionless SP parameter $SP=B/\sigma$. It is the intermonomer electronic coupling that drives the excitation transfer. In nearest-neighbor approximation and neglecting end effects, this is given simply by $B=2V$, where $V=V_{n,n+1}$ is assumed to be independent of n . In this section (although not throughout the paper), we will adopt the standard model of identical harmonic potentials in the ground and excited electronic states. The electronic coupling then is measured in units of $\hbar\omega$, the vibrational quantum. In this model the dimensionless Huang–Rhys parameter X is a direct measure of the strength of intramonomer vibronic coupling. This parameter also decides the energy width $\sigma=\sqrt{X}\hbar\omega$ of the monomer absorption spectrum through the Poissonian distribution of FC factors [Eq. (1)]. Hence the ratio $2V/\sigma$ is the SP parameter value and a measure of the excitonic coupling strength. Also it is meaningful to express time in units of T_{el} , the typical time of intermonomer excitation transfer, given in this case by $(\hbar/2V)$. In Table I the relations between the quantities used in the analysis are summarized.

For short aggregates it is important to note that, for a circular aggregate, interference between counterpropagating wavepackets occurs after the excitation wave travels 180°

around the circle. Similarly, for a linear aggregate, reflection at the end points leads to interference with the primary wave. To avoid such effects, here we will concentrate on the short-time behavior, considering the excitation wave rolling out from monomer 0 and showing $P_{n0}(t)$ only up to times where the primary wave front reaches the penultimate monomer. Typical results of full calculations for $P_{n0}(t)$ according to Eq. (10) are presented in Figs. 2–4. The dimension of the basis states of Eq. (9) is given by $D=Nn_e n_g^{N-1}$, where n_e is the number of vibrational states included for the excited electronic state and n_g is for the ground electronic state. For this reason, for fixed N and n_e , the values of n_g must be rather limited to make the problem numerically tractable. Nevertheless, for small aggregates, say $N=5$ with n_e as large as 9, we found that we could run calculations with n_g of up to 4. Of course, the values of n_g and n_e necessary for convergence depend strongly on the Huang–Rhys factor; here we used $X\leq 1$. In test calculations, we found that with $n_g=4$ and $n_e=9$, the time-dependent excitation probability, even in the intermediate coupling regime, is well converged within the time range considered. We note that, as said in Ref. 42, the CES approximation is exactly equivalent to performing a basis set expansion with the restriction that $n_g=1$. Hence, calculations presented in this subsection for $n_g=1$ will be denoted as the CES approximation. First we consider a circular aggregate of five monomers ($N=5$), numbered along the aggregate beginning with the initially excited monomer 0. In Fig. 2 left, $P_{n0}(t)$ is plotted for extreme strong coupling of $2V=10$. Actually on each curve three results, for increasing vibronic coupling, $X=0, 0.3$, and 1.0 are plotted but they are undistinguishable for this coupling strength. Note that $X=0$ gives only the zero-zero vertical transition and so gives results identical to the purely electronic case. Then, as one might expect, there is a smooth movement of the excitation peak along the monomer chain as time progresses. The popu-

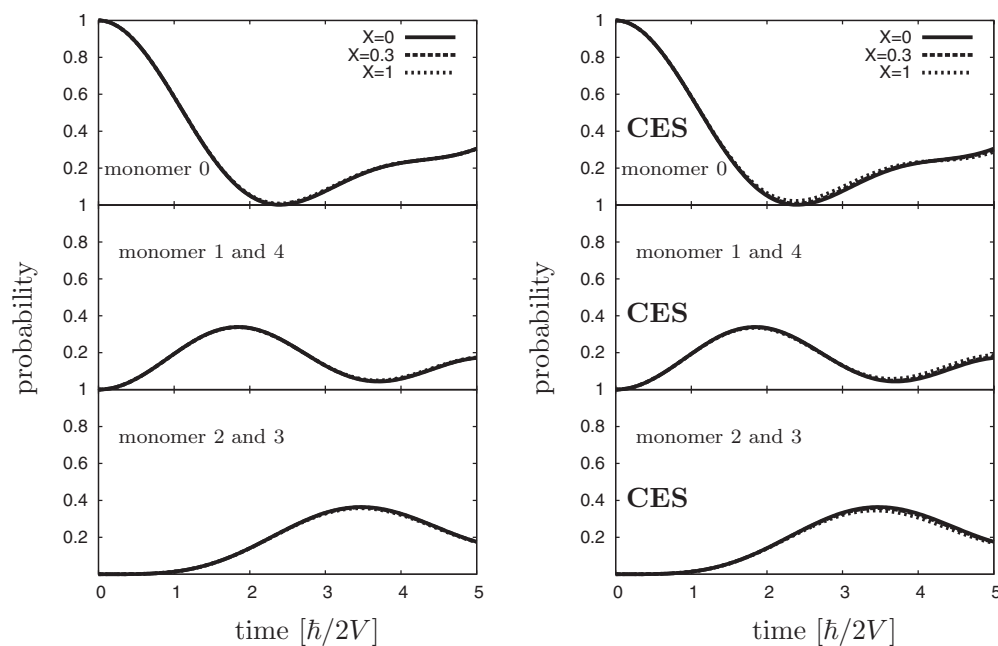
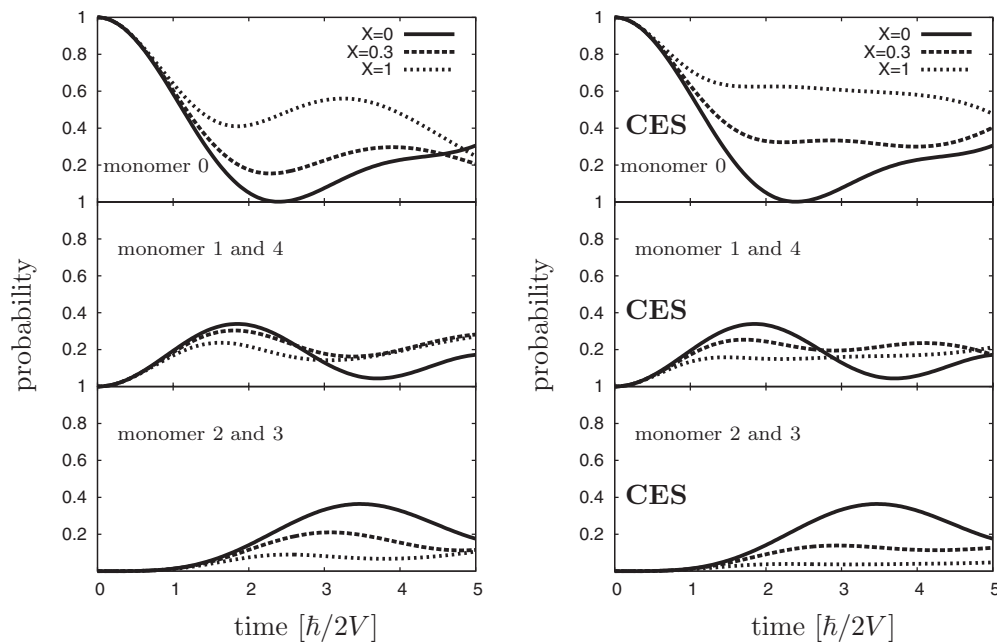
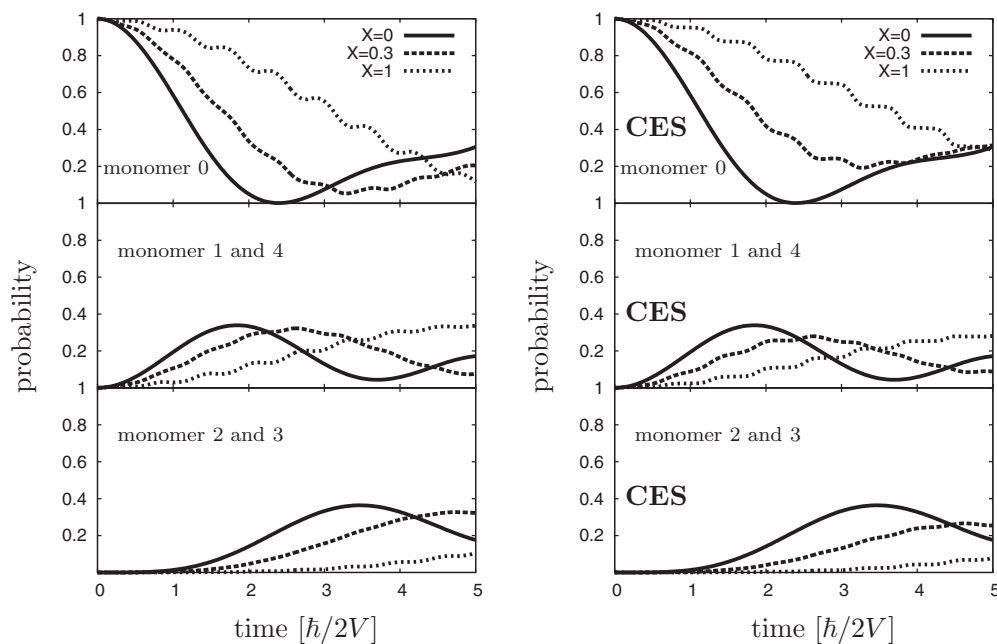


FIG. 2. Excitation probability as a function of time, in units of T_{el} for a ring with $N=5$. Left figure: with $n_g=4$; right figure: CES result ($n_g=1$). Here $2V=10\hbar\omega$ and $n_e=9$. The values for X are indicated in the figures.

FIG. 3. Same as Fig. 2 but with $2V=1\hbar\omega$.

448 lation of monomer 0 is roughly halved after a time T_{el} , falls
 449 to zero but then revives at later times. As we shall see, this
 450 oscillatory behavior of the excitation probability is typical of
 451 strong coupling. The CES results for $n_g=1$ on the right set of
 452 figures in Fig. 2 are shown and one notes that in strong
 453 coupling, exact and CES approximation are in almost perfect
 454 agreement. The intermediate coupling case is where vibronic
 455 effects are most pronounced and in Fig. 3 the $P_{n0}(t)$ are
 456 shown for the same parameters as in Fig. 2 except that now
 457 $2V=1.0$. Since the $X=0$ case is purely electronic, on the
 458 scaled time $(2V/\hbar)t$, these curves are identical to those in
 459 Fig. 2. Now, however, as X increases, there occurs a pro-
 460 nounced slowing down of excitation transfer so that about

50% probability remains on monomer 0 and only about 10%
 reaches monomer 3. Although the curves in Fig. 3 (left) are
 for $n_g=4$, the $n_g=1$ CES results in Fig. 3 (right) are in fair
 qualitative agreement even for this case of intermediate
 coupling. Again from Fig. 3 (right), one sees an overall slowing
 of transfer with increasing X , i.e., with stronger vibronic
 coupling. The weak electronic coupling case is shown in Fig. 4.
 Here one sees clearly the damping effect of vibronic
 coupling on the rate of excitation transfer. In Fig. 4 (bottom),
 in contrast to the strong-coupling case in Fig. 2 (bottom),
 one sees that monomer 3 is only maximally $\sim 10\%$ excited for
 $X=1.0$, whereas in strong coupling, this value is around 30%.
 The CES results are given in Fig. 4 (right) and again are in

FIG. 4. Same as Fig. 2 but with $2V=0.1\hbar\omega$, i.e., weak electronic coupling.

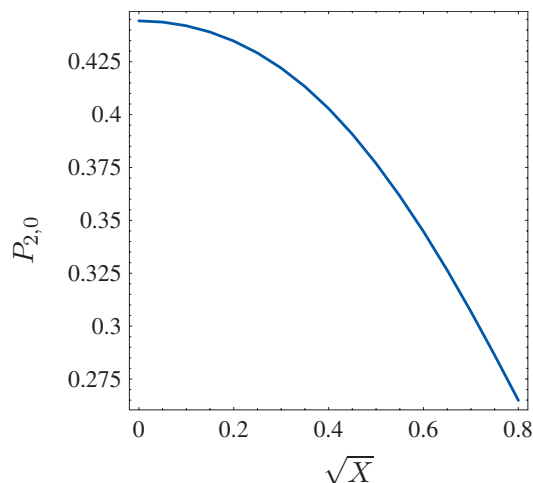


FIG. 5. Magnitude of the first maximum at monomer 2 as a function of \sqrt{X} with $2V=2$ for a linear chain with $N=5$. The calculation has been made with $n_g=2$ and $n_e=5$.

initial monomer arbitrarily the number $m=0$ as fixed value. **507**
Then we transform from the localized monomer number n to **508**
the exciton number k , i.e., **509**

$$G_{n0}(E) = \langle \pi_n | G(E) | \pi_0 \rangle = \frac{1}{\sqrt{N}} \sum_k e^{-ikn} \langle k | G(E) | \pi_0 \rangle. \quad (20) \quad \mathbf{510}$$

The interaction matrix element in Eq. (15) is transformed **511**

$$V_{mm'} = \frac{1}{N} \sum_{kk'} e^{-ikn+ik'n'} V_{kk'}. \quad (21) \quad \mathbf{512}$$

If we consider all monomers identical, then, for a ring or **513**
linear chain of monomers, it is easily seen that $V_{kk'}$ is diag- **514**
onal, i.e., **515**

$$V_{mm'} = \frac{1}{N} \sum_k e^{-ik(n-n')} V_k. \quad (22) \quad \mathbf{516}$$

Substituting Eqs. (22) and (20) into Eq. (15) leads to **517**

$$\langle k | G(E) | \pi_0 \rangle = g_0 + g_0 V_k \langle k | G(E) | \pi_0 \rangle. \quad (23) \quad \mathbf{518}$$

To obtain a tractable form for $\langle k | G(E) | \pi_0 \rangle$, at this stage it is **519**
convenient to make the CES approximation in which g_0 in **520**
the second term on the right hand side of Eq. (23) is approxi- **521**
mated by the ground-state average, i.e., **522**

$$g_0 \rightarrow \langle \sum_g |g_0\rangle | \sum_g \rangle \equiv \langle g_0 \rangle. \quad (24) \quad \mathbf{523}$$

Then, from Eq. (23) one finds $\langle k | G(E) | \pi_0 \rangle = g_0 (1 - \langle g_0 \rangle V_k)^{-1}$ **524**
so that the operator $G_{n0}(E)$ can be written as **525**

$$G_{n0}(E) = \frac{1}{N} \sum_k e^{ikn} \frac{g_0}{1 - \langle g_0 \rangle V_k}. \quad (25) \quad \mathbf{526}$$

In fact, since all monomers are identical, we can henceforth **527**
drop the subscript 0 on $\langle g_0 \rangle$. Within the spirit of the CES, the **528**
operator g_0 also will be represented on the basis of vibra- **529**
tional states of the aggregate with one monomer electroni- **530**
cally excited and all others in the ground electronic and vi- **531**
brational states, i.e., **532**

$$|\alpha\rangle \equiv |\alpha, 0, \dots, 0\rangle = |\chi_0^\alpha\rangle \prod_{n \neq 0} |\xi_n^0\rangle, \quad (26) \quad \mathbf{533}$$

where $|\chi_0^\alpha\rangle$ is the α th excited vibrational state in the upper **534**
monomer potential curve. Then we have **535**

$$g_0(E) = \frac{1}{E - H_{\text{mon}} + i\delta} = \sum_\alpha \frac{|\alpha, 0, \dots, 0\rangle \langle \alpha, 0, \dots, 0|}{E - E_\alpha + i\delta}, \quad (27) \quad \mathbf{536}$$

where $E_\alpha - \epsilon_{el}$ is the energy of the vibrational state α in the **537**
upper potential curve and ϵ_{el} is the monomer electronic ex- **538**
citation energy. Performing the average (24), one has **539**

$$\langle g \rangle = \sum_\alpha \frac{|f_0^\alpha|^2}{E - E_\alpha + i\delta}, \quad (28) \quad \mathbf{540}$$

where $f_0^\alpha = \langle \chi^\alpha | \xi^0 \rangle$ is the FC overlap between the initial and **541**
the final monomer vibrational states. Substituting Eqs. (27) **542**
and (28) into Eq. (25) gives a closed form expression for **543**
 G_{n0} , i.e., **544**

474 excellent agreement with the exact results. For weak cou-
475 pling, the same agreement was found between absorption
476 spectra calculated by full diagonalization and in CES
477 approximation.⁴² A more quantitative picture of the depen-
478 dence of excitation transfer on X is given in Fig. 5. Here we
479 use the magnitude of the maximum of the first wave front,
480 i.e., the first maximum of the time-dependent excitation
481 probability, at a particular monomer as a measure of the ef-
482 ficiency of excitation propagation. In Fig. 5 the value of the
483 first maximum to reach monomer 2 (when initially starting at
484 monomer 0) is plotted as a function of \sqrt{X} for fixed $2V=2$.
485 Again one sees a strong drop in this probability of excitation
486 as the vibronic coupling parameter increases.

487 IV. TIME PROPAGATOR IN THE CES APPROXIMATION

488 A. A single IM vibration: Analytical results

489 Now we discuss the excitation transfer process solely in
490 the CES approximation since this allows the derivation of
491 simple analytic forms for the excitation propagation prob-
492 ability $P_{n0}(t)$ both in the case of strong and of weak cou-
493 plings. Furthermore, we can perform numerical calculations
494 for very long aggregates. In discussing excitation transfer
495 analytically, it is also convenient to introduce delocalized
496 exciton electronic states defined as

$$|k\rangle = \frac{1}{\sqrt{N}} \sum_n e^{ikn} |\pi_n\rangle, \quad (19) \quad \mathbf{497}$$

498 where $k=2\pi/N(j-1)$ and j runs from 1 to N and we have
499 assumed cyclic boundary conditions. Although not necessary,
500 the condition of replacing the linear chain by a circular ag-
501 gregate will be made in this section since the analytical ex-
502 pressions obtained are simpler than for a finite linear chain,
503 where end effects lead to more complicated formulas.

504 In order to calculate $G_{n0}(t) | \Sigma_g \rangle$ in Eq. (10), we consider
505 first the Fourier transform to energy space, i.e., the state
506 $G_{n0}(E) | \Sigma_g \rangle$, where $G_{n0}(E)$ satisfies Eq. (15). We assign the

$$G_{n0}(E) = \frac{1}{N} \sum_k e^{ikn} \sum_\alpha \frac{|\alpha, 0, \dots, 0\rangle \langle \alpha, 0, \dots, 0|}{E - E_\alpha + i\delta - V_k \sum_\beta |f_0^\beta|^2 \frac{E - E_\alpha + i\delta}{E - E_\beta + i\delta}}. \quad (29)$$

545

546 This closed form result (29) can be evaluated easily in two
547 limits. First, in strong coupling where $2V$ is much larger than
548 the width of the monomer vibrational band, represented by
549 the width of the FC distribution $|f_0^\beta|^2$, we can replace E_β by
550 its average value $\bar{\epsilon}$. Furthermore, since when the probability
551 (10) is formed, the sum over α is also limited to the spread of
552 the monomer vibrational band, we can also replace E_α by the
553 same average value. This corresponds to assuming that the
554 vibrational states which carry oscillator strength are so
555 closely spaced in energy compared to the exciton bandwidth
556 that they can be replaced effectively by a single level at the
557 mean energy $\bar{\epsilon}$. Then, since

$$\sum_\beta |f_0^\beta|^2 = 1, \quad (30)$$

558

559 we have

$$G_{n0} \approx \frac{1}{N} \sum_k e^{ikn} \frac{\mathbb{1}_u}{E - \bar{\epsilon} - V_k + i\delta}, \quad (31)$$

560

561 where $\mathbb{1}_u$ is the unit operator in the space of upper vibrational
562 states of monomer 0. Our strong-coupling criterion is exactly
563 that of Simpson and Peterson³⁸ and apart from the unit op-
564 erator the result (31) is exactly that obtained by ignoring
565 vibrations altogether.

566 From Eq. (31), one obtains

$$G_{n0}(t) = \mathbb{1}_u \frac{1}{N} \sum_k e^{ikn} \exp\left(-\frac{i}{\hbar}(\bar{\epsilon} + V_k)t\right) \quad (32)$$

567

568 and from Eq. (10) the transfer probability

$$P_{n0}(t) = \left| \frac{1}{N} \sum_k e^{ikn} \exp\left(-\frac{i}{\hbar}(\bar{\epsilon} + V_k)t\right) \right|^2, \quad (33)$$

569

570 where again we used Eq. (30).

571 In nearest-neighbor coupling V_k has the simple form V_k
572 $= 2V \cos k$. Then, dropping the unit operator from Eq. (32)
573 since it disappears in the probability (33), we have the purely
574 electronic result

$$G_{n0}(t) = \frac{1}{N} \sum_j \exp\left[i \frac{2\pi}{N} jn - \frac{i}{\hbar} \left(\bar{\epsilon} + 2V \cos\left(\frac{2\pi}{N}j\right) \right) t \right]. \quad (34)$$

575

576 Using the generating function for Bessel functions

$$e^{-iz \cos \varphi} = \sum_{l=-\infty}^{\infty} (-i)^l J_l(z) e^{il\varphi}, \quad (35)$$

577

578 one obtains

$$G_{n0}(t) = \frac{1}{N} e^{-i\hbar\bar{\epsilon}t} \sum_{l=-\infty}^{\infty} (-i)^l J_l\left(\frac{2V}{\hbar}t\right) \sum_j e^{i(2\pi/N)j(n-l)}. \quad (36)$$

579

AQ: 580 The monomers on the circular aggregate are enumerated
#7

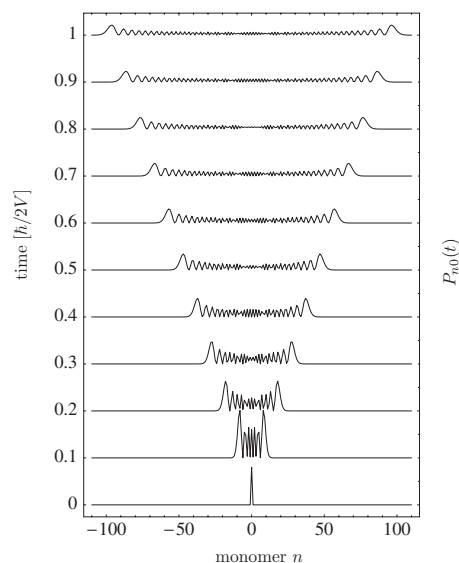


FIG. 6. The probability $P_{n0}(t)$ for strong coupling as a function of n at the times indicated. For better visibility, $P_{n0}(t=0)$ has been reduced to 8% of its real value.

$$N \text{ odd: } -\frac{N-1}{2} \leq n \leq \frac{N-1}{2}, \quad (37)$$

$$N \text{ even: } -\frac{N}{2} + 1 \leq n \leq \frac{N}{2} \quad \text{or} \quad -\frac{N}{2} \leq n \leq \frac{N}{2} - 1. \quad (38)$$

To evaluate Eq. (33) further, we consider the limit $N \rightarrow \infty$ to
obtain the simple result

$$P_{n0}(t) = J_n^2\left(\frac{2V}{\hbar}t\right). \quad (38)$$

This is the result of Merrifield³⁹ for purely electronic excita-
tion transfer on an infinite linear aggregate. Hence we have
shown that, with vibrations, the strong-coupling limit gives
the purely electronic result, as one might expect. Note that
the time defined by $T_{el} = (\hbar/2V)$ emerges as the natural scale
unit for time and corresponds to the electronic excitation
transfer time between adjacent monomers when vibrations
are not coupled. In Fig. 6, $P_{n0}(t)$, according to Eq. (38), is
plotted for a succession of times as a function of monomer
number. Then one sees that the leading maximum of the
distribution moves roughly linearly with time.

The probability $P_{n0}(t)$ is plotted in Fig. 7 for the case

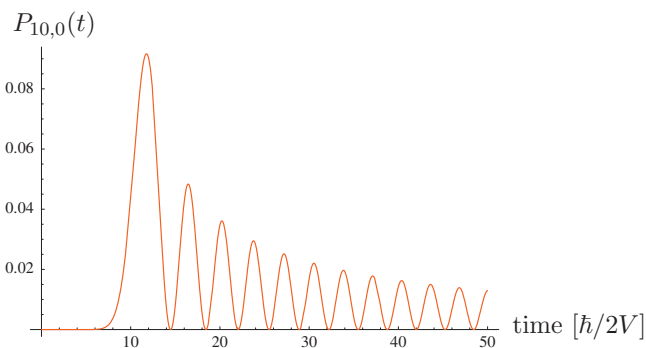


FIG. 7. The probability $P_{10,0}(t)$. The time is in units of $(\hbar/2V)$.

599 $n=10$ and one sees clearly the oscillatory nature of excitation
600 and de-excitation of a given monomer. This explains the os-
601 cillations seen in the numerical results in Fig. 2. One also
602 notes that, due to a simple property of the Bessel functions,
603 the first excitation peak reaches the monomer n at a time
604 which is close to n units of the fundamental time T_{el} , as can
605 be seen in Fig. 7 for the case $n=10$. This property is dis-
606 cussed more fully in Sec. IV B. The mean square displace-
607 ment is given by the average

$$\overline{n^2(t)} = \sum_{n=0}^{\infty} n^2 P_{n0}(t) = \frac{V^2}{\hbar^2} t^2. \quad (39)$$

609 If we define $\tilde{n} \equiv (\overline{n^2(t)})^{1/2}$ and the mean propagation velocity
610 $d\tilde{n}/dt$, we see that exciton propagation is at constant velocity
611 $d\tilde{n}/dt = (V/\hbar)$ away from the initial site $n=0$ of excitation.

612 The second simple analytic limit of Eq. (29) is provided
613 by the case in which the electronic coupling $2V$ is so small
614 that mixing of the vibronic levels in the upper electronic
615 state can be ignored in the propagator. Then only the diago-
616 nal term $\beta = \alpha$ in the denominator of Eq. (29) is considered to
617 give

$$G_{n0} \approx \frac{1}{N} \sum_k e^{ikn} \sum_{\alpha} \frac{|\alpha, 0, \dots, 0\rangle \langle \alpha, 0, \dots, 0|}{E - E_{\alpha} - V_k |f_0^{\alpha}|^2 + i\delta}. \quad (40)$$

619 Thus, following the steps leading from Eq. (31) to Eq. (38),
620 one has

$$G_{n0}(t) = \sum_{\alpha} |\alpha\rangle \langle \alpha| e^{-i\hbar E_{\alpha} t} (-i)^n J_n \left(\frac{2V}{\hbar} |f_0^{\alpha}|^2 t \right) \quad (41)$$

622 and

$$P_{n0}(t) = \sum_{\alpha} |f_0^{\alpha}|^2 J_n^2 \left(\frac{2V}{\hbar} |f_0^{\alpha}|^2 t \right). \quad (42)$$

624 This result was obtained by Bierman⁴⁰ using a somewhat
625 more complicated approach than the Green's function
626 method adopted here. Again, one has an oscillatory behavior
627 of the excitation probability with time, in agreement with the
628 weak-coupling numerical results shown in Fig. 4. The result
629 of Eq. (42) can be interpreted simply. In this extreme weak-
630 coupling limit each monomer vibronic level splits into its
631 own exciton band of N levels on aggregate formation but the
632 individual vibronic exciton bands do not overlap. Then exci-
633 tation transfer occurs resonantly between individual vibronic
634 levels so that the fundamental transfer time is reduced by the
635 factor $|f_0^{\alpha}|^2$ compared to Eq. (38). Correspondingly, the exci-
636 ton bandwidth for excited vibrational state α is $2V|f_0^{\alpha}|^2$, as
637 can be inferred from Eq. (40). From Eq. (42), the average
638 monomer $(\overline{n^2(t)})^{1/2}$ reached at time t is given by the equation

$$\overline{n^2(t)} = \frac{V^2}{\hbar^2} t^2 \sum_{\alpha} |f_{\alpha 0}|^6. \quad (43)$$

640 This result can also be understood in a simple way. Since
641 each vibronic level is independent, from Eq. (39) one would
642 have, for level α

$$\overline{n_{\alpha}^2(t)} = \frac{V^2 |f_0^{\alpha}|^4}{\hbar^2} t^2. \quad (44)$$

Then summing over all levels one has

$$\overline{n^2(t)} = \sum_{\alpha} \overline{n_{\alpha}^2(t)} p_{\alpha}, \quad (45)$$

where p_{α} is the probability of excitation of level α . However
 p_{α} is just given by $|f_0^{\alpha}|^2$ so from Eqs. (44) and (45) one
directly finds the result [Eq. (43)].

From Eq. (43) one has that the constant mean propaga-
tion velocity in this case is $d\tilde{n}/dt = (V/\hbar)(\sum_{\alpha} |f_0^{\alpha}|^6)^{1/2}$. Since it
is readily seen that $\sum_{\alpha} |f_0^{\alpha}|^6 < 1$, one has the result that even
though excitation transfer is at constant velocity, the pres-
ence of vibrations leads a lower velocity of propagation than
when they are ignored. We note that the simple SP definition
of weak coupling is not really appropriate here. In the limit
corresponding to the result [Eq. (42)], one has rather that the
vibrational level spacing must be greater than the maximum
value of the vibronic exciton bandwidth $2V|f_0^{\alpha}|^2$. This is an
additional condition to the SP criterion.

B. A single IM vibration: Numerical results

Since for the chosen basis the dimension of a full nu-
merical propagation contains the factor n_g^{N-1} , it is not pos-
sible to perform full calculations on large aggregates. Happi-
ly, however, we have seen that the CES approximation
with $n_g=1$, gives excellent results for weak and strong cou-
pling and qualitatively good results for intermediate cou-
pling. Then we can use formula (29) for $G_{n0}(E)$ to construct
numerically $G_{n0}(t)$ and hence calculate $P_{n0}(t)$. Formula (29)
depends implicitly on N through the summation over exciton
index k . Actually, since the use of formula (29) gives the
same results as the numerical procedure with restriction to
 $n_g=1$, it is simpler to adopt the latter method of calculation.

First let us consider the velocity of the wave front. We
return to the purely electronic result [Eq. (38)] for an infinite
chain of monomers. As one sees from Fig. 7, $P_{n0}(t)$ is oscil-
latory and the time at which a maximum is reached is given
by $dP_{n0}(t)/dt=0$. The monomer number n over the time of
arrival of the first wave front maximum at this monomer is
plotted in Fig. 8. The speed is rapidly a constant, the wave
traveling over ten monomers in around ten time units, i.e.,
the speed is $2V/\hbar$, which is just twice the mean velocity
 $d\tilde{n}/dt$. Again we emphasize that the purely electronic result
in Fig. 8 is obtained in the vibronic case for $X=0$ and corre-
sponds to the extreme strong-coupling limit.

The case of weak coupling and $N \rightarrow \infty$ gives the analytic
result of Eq. (42). Here, a linear relation between n and t is
also predicted, as confirmed by the plot in Fig. 9. However,
what is noteworthy is the large decrease in the velocity of the
wavepacket caused by the presence of FC factors in Eq. (42).
In Fig. 9, one sees that a displacement over ten monomers
now requires about 25 time units compared to 10 in the pure
electronic case in Fig. 8.

Within the weak-coupling limit, it is useful also to ex-
amine the X dependence of the $v=n/t$ constant velocity re-
sult. One can show that the dependence follows the analytic
form $v=n/t=2V/\hbar e^{-X}$, indicating a strong reduction in ve-

AQ:
#8

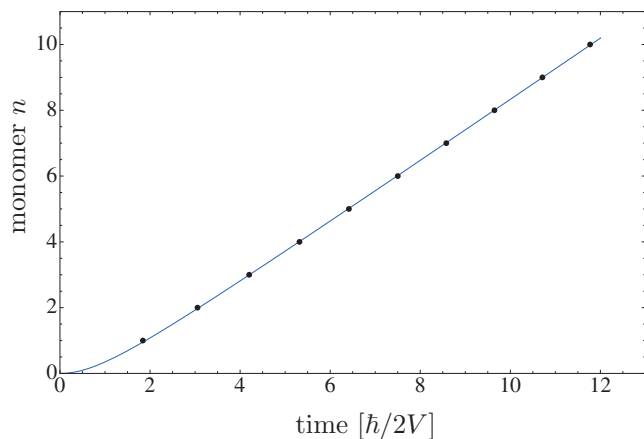


FIG. 8. Time of arrival of the first wave front maximum at monomer n . For $X=0$, i.e., strong coupling.

697 locity as the vibronic coupling increases. This is in qualita-
698 tive agreement with Eq. (43) when the rms value \tilde{n}/t is
699 evaluated for the case of a Poissonian distribution of FC
700 factors.

701 Finally, there is the intermediate coupling case. The $n(t)$
702 curve for this case is shown in Fig. 10 for $2V=2$ and X
703 $=0.64$. Here a new feature arises in that there are apparent
704 discontinuities in the propagation. A closer inspection of the
705 individual $P_{n0}(t)$ curves (Fig. 11) shows that this is a new
706 feature due to the strong vibronic coupling, namely, that the
707 original leading wave front dies out in time and is replaced
708 by the second as “leading” maximum. This smearing of the
709 dominant first maximum is a general feature of vibronic cou-
710 pling. It occurs around $t=11$ in Fig. 11 and gives rise to an
711 apparent delay in arrival of the wave front. By comparison
712 with the strong-coupling case in Fig. 6, one sees also that
713 when vibronic coupling is present, the wavepacket is spread
714 more evenly among the monomers, indicating that vibra-
715 tional states of the electronically excited monomer take
716 longer to transfer their energy.

717 C. Coupling to a vibrational continuum: 718 Numerical results

719 The final and most important step is to include coupling
720 to the continuous distribution of EM and thereby achieve a

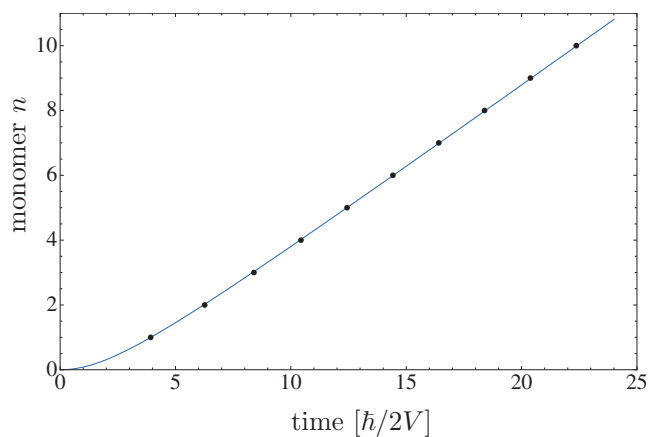


FIG. 9. Time of arrival of the first wave front maximum at monomer n . For weak coupling ($V=0.1$) and $X=0.64$.

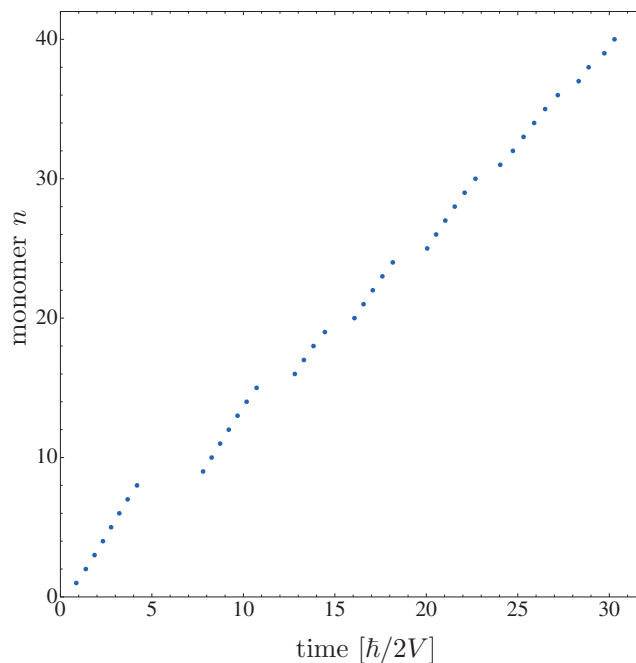


FIG. 10. Time of arrival of the first wave front maximum at monomer n . With $X=0.64$ and intermediate coupling.

more realistic description of the coupling of the electronic 721
excitation to the vibrations of the surroundings, while still 722
retaining the effect of the primary coupling to the IM vibra- 723
tions. In the standard approach [see point (1) in Sec. I] vibra- 724
tions are ignored explicitly and calculations are per- 725
formed for a particular choice of monomer electronic 726

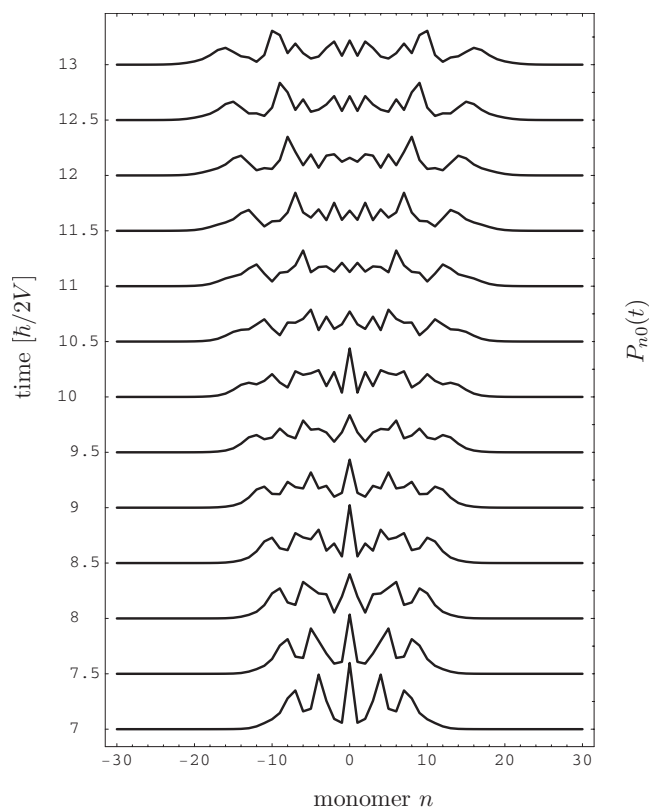


FIG. 11. The distribution $P_{n0}(t)$ as a function of monomer position n shown at successive times.

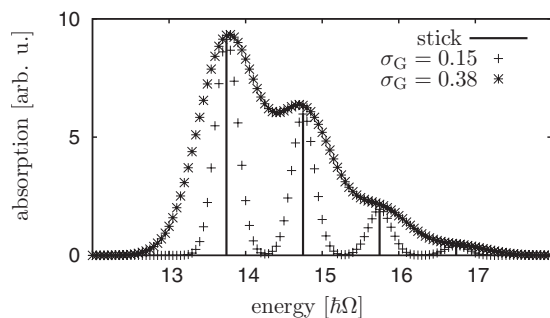


FIG. 12. Poissonian with $X=0.61$ used to fit the measured monomer absorption spectrum of the PIC dye of Ref. 43. Vertical lines, stick spectrum; crosses, convoluted with a Gaussian of width $\sigma_G=0.15$; and stars, with $\sigma_G=0.38$. The energy axis and the values for σ_G are given in units of the stick spacing $\hbar\Omega$.

mer as a function of time. The figures in the first row [Figs. 770 13(a)–13(c)], show an extreme strong-coupling case. The 771 pattern is that of Fig. 6 and is the analytic Bessel function 772 result for pure electronic excitation given by Eq. (38). Also 773 shown on the figure as a continuous line is the displacement 774 $\tilde{n}(t)=(\tilde{n}^2(t))^{1/2}$ demonstrating the linear behavior expected. 775 This regular oscillatory pattern is identical in Figs. 776 13(a)–13(c), showing that the extreme strong-coupling, 777 purely electronic result has been achieved. However, already 778 for $2V=10$, corresponding to a SP parameter of $SP\approx 12$, one 779 sees deviations from the Merrifield result, as shown in Figs. 780 13(d)–13(f). Although the pattern is still regular, at larger 781 times the second maximum becomes more pronounced than 782 the first and there is a slowing of the velocity of propagation, 783 indicated by the decreasing slope of the \tilde{n} line, which be- 784 comes more pronounced as the continuous width σ_G in- 785 creases. This trend is emphasized as the coupling becomes 786 somewhat weaker [Figs. 13(g)–13(i)] with $2V=5$ corre- 787 sponding to $SP\approx 6$. In the course of time, the probability 788 becomes more smeared out over the whole aggregate, al- 789 though regularity is still discernible. Note that the width of 790 the monomer absorption spectrum is mainly determined by 791 the width stemming from the primary vibrational mode with 792 $X=0.61$. The convolution with the continuous Gaussian 793 changes the overall width only slightly. For example, in the 794 case $2V=5$ one has a SP parameter $SP=6.4$ for the stick 795 spectrum and $SP=5.7$ for the spectrum with $\sigma_G=0.38$. 796

The cases in Figs. 13(j)–13(l) approach an intermediate 797 coupling, with $SP\approx 3$. One sees, for the stick spectrum in 798 Fig. 13(j), a general smearing out of an irregular probability 799 pattern and a pronounced concentration of probability re- 800 maining around the origin. This tendency increases dramati- 801 cally as the continuous width is increased [Figs. 13(k) and 802 13(l)]. Although the propagation velocity (\tilde{n}/t) reduces con- 803 siderably with the width, it still remains finite, indicating that 804 there is still a continuing transfer of probability along the 805 chain. However, comparison of Figs. 13(j)–13(l) shows for 806 the first time the new effect arising from transition to a con- 807 tinuous spectrum or, equivalently, strong coupling to external 808 modes. There is a marked tendency, not evident in the case 809 of a stick monomer spectrum, for excitation to remain 810 trapped on the first few monomers. 811

The trapping of excitation becomes increasingly pro- 812 nounced when $2V$ is reduced to give intermediate and weak 813 coupling, and the width σ_G is increased. This is shown in 814 Figs. 13(m)–13(r). For $2V=1$, the stick spectrum gives ir- 815 regular propagation but for $\sigma_G=0.38$ [Fig. 13(o)], there is a 816 complete collapse of propagation and \tilde{n} becomes constant in 817 time. Finally, for the case of weak coupling the transition to 818 a continuous spectrum becomes even more dramatic. Figures 819 13(p)–13(r) are for the case $SP=0.6$. For the stick spectrum 820 [Fig. 13(p)], constant velocity propagation is recovered and 821 the pattern of probability change is becoming regular, corre- 822 sponding to a slow approach to the Bierman, case of Eq. 823 (42). By contrast, even for $\sigma_G=0.15$, when the spectrum of 824 the monomer is continuous, excitation remains trapped near 825 the origin and increasingly so as the continuous width in- 826 creases. 827

One can question the physical origin of the trapping 828

727 transition energies and/or electronic intermonomer coupling
728 strengths. Then, in the final step, an average is performed
729 over different realizations of this disorder. In this step, the
730 statistical distribution of transition energy (diagonal disorder)
731 and coupling strength (nondiagonal disorder) are taken as fit
732 parameters. Here we seek to make contact with experiment
733 by using the measured monomer continuous spectrum as in-
734 put. Specifically, we include a primary IM vibration but then
735 we clothe each vibronic level of the monomer with a se-
736 quence of densely packed discrete EM transitions, giving rise
737 to an effective continuum of vibronic transitions. As with
738 statistical disorder, this procedure leads to a continuum of
739 possible transition energies along the chain and, through the
740 continuous variation of FC factors, to a continuous distribu-
741 tion of coupling strength between adjacent monomers.
742 Again, as with statistical disorder, the character of this as-
743 sumed continuous distribution is arbitrary. However, here we
744 choose the distribution specifically to reproduce the experi-
745 mental isolated-monomer continuous absorption spectrum.
746 An example is shown in Fig. 12, where we fit the measured
747 continuous spectrum of the PIC monomer.⁴³ The experimen-
748 tal data suggest a single (effective) primary IM mode shown
749 by the fitted discrete “stick” spectrum. In the next step, each
750 of the four vibronic peaks is folded with a Gaussian continu-
751 ous distribution of width σ_G . Shown in Fig. 12 are the cases
752 $\sigma_G=0.15$ and $\sigma_G=0.38$ (in units of the stick spacing $\hbar\Omega$).
753 This latter value gives an excellent reproduction of the ex-
754 perimental spectrum (not shown).^{43,44} Since the vibrational
755 basis only manifests itself in the Hamiltonian equation (17)
756 through the monomer vibrational energies and the corre-
757 sponding FC factors and since the monomer absorption spec-
758 trum provides these factors, the remaining step is simply to
759 take the FC distribution in Fig. 12 as a quasicontinuous dis-
760 tribution. The $P_{n0}(t)$ calculated using the continuous distri-
761 butions of FC factors is shown in Fig. 13. Here we took 120
762 discrete values to represent the continuous distribution in
763 Fig. 12. The aggregate in this case is a linear chain of 50
764 monomers with monomer 0 placed at one end and only
765 propagation over one-half of the aggregate displayed for
766 times for which the other end has not been reached. The
767 values of $2V$ and the width σ_G of the individual Gauss peaks
768 is indicated on the figures. In color-coded form, the figures
769 show the electronic excitation probability of a given mono-

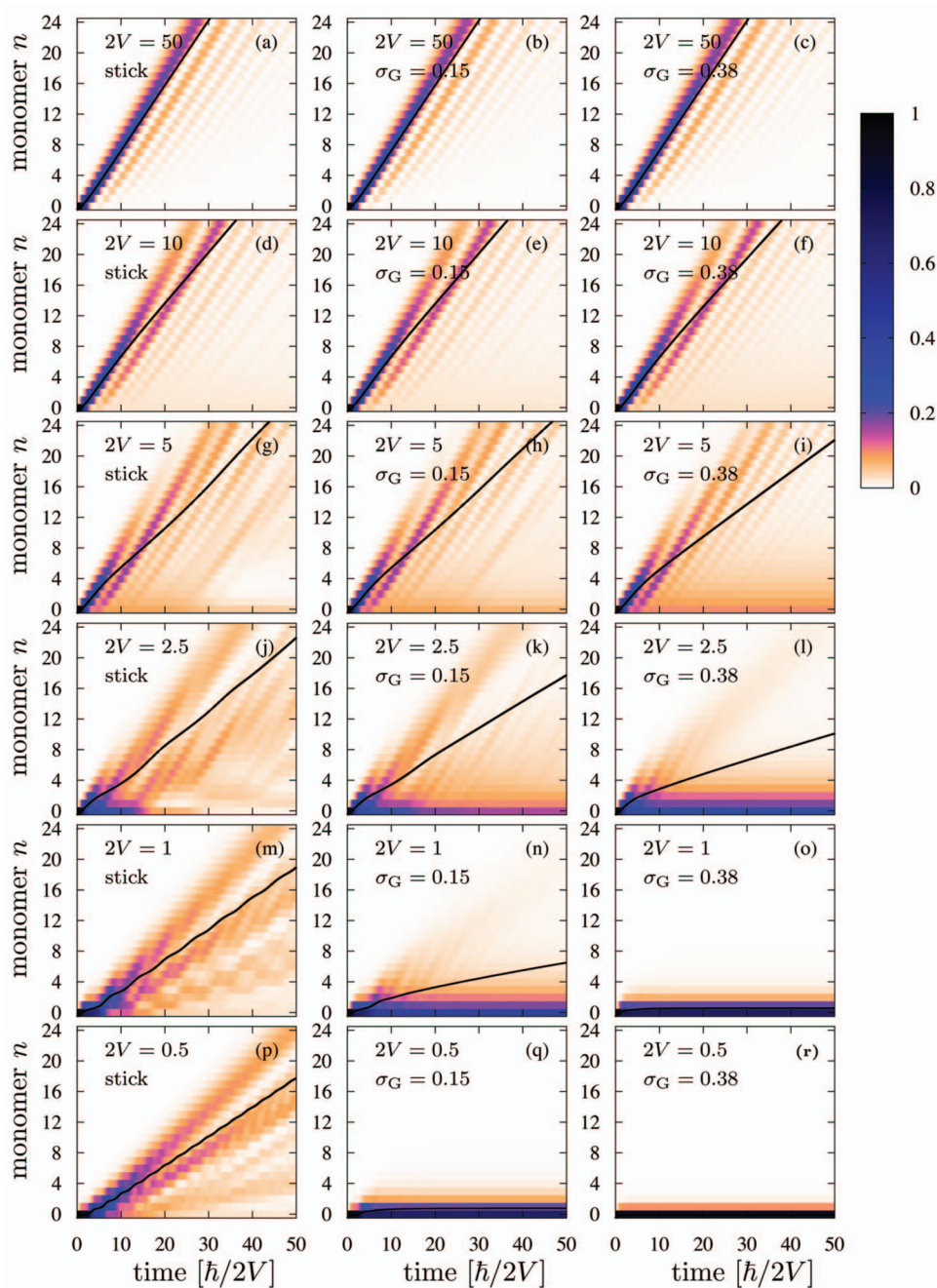


FIG. 13. Probability $P_{n0}(t)$ that monomer n is electronically excited at time t . The aggregate is a linear chain of $N=50$ monomers (only one-half of the aggregate is shown here). The values for $2V$ and the convolution width σ_G of the monomer spectrum are indicated on the figures. The continuous line shows $\tilde{n}(t)$.

mechanism. As we show explicitly in Sec. IV D, this is readily understood. A discrete set of oscillator eigenstates in the upper potential, giving rise to a stick spectrum, requires the establishment of repeated oscillation, in principle, for an infinite time, in the upper potential well. Clearly, any coupling to other modes leads to a broadening of the absorption line. Coupling to very many densely packed EM leads to an effective continuum broadening. In the time picture, this can be mimicked by considering that a time-dependent vibrational wavepacket is formed in the upper state. If the wavepacket reflects back and forth many times in a potential well, vibrational eigenstates are formed and the absorption spectrum is structured. A structureless absorption continuum would then correspond to the extreme situation that the wavepacket moves out of the region of overlap with vibrational states of the ground electronic state and does not re-

turn [see Fig. 1(b)]. In this way the coupling to EM is represented by an effective repulsive BO potential in the upper state. The electronic excitation can only be transferred during the time when there is overlap between ground-state and excited-state vibrational wavepackets. For longer times the FC factor is zero and the excitation remains trapped. In the following we derive a simple analytic model which explains the trapping phenomenon.

D. Coupling to a vibrational continuum: The Magee–Funabashi approximation

We have seen from the numerical results of Sec. IV C that the transition to a continuous spectrum has a profound effect on the character of exciton propagation. In particular, for intermediate coupling, we observe a trapping of the ex-

859 citon at a time characteristic of the electronic coupling
860 strength and the width of the vibronic spectrum, which itself
861 is a measure of the strength of the intramonomer vibronic
862 coupling. Now we will show how an approximate analytic
863 result can be derived in CES approximation, which allows a
864 simple physical interpretation of the trapping predicted by
865 the numerical results of Sec. IV C to be given. In Appendix
866 A it is shown that the probability that electronic excitation
867 has reached monomer n is given by,

$$868 \quad P_{n0}(t) = |J_n(\gamma(t))|^2, \quad (46)$$

869 where

$$870 \quad \gamma(t) = (2V/\hbar) \int_0^t F(t') dt'. \quad (47)$$

871 One notes that the argument $\gamma(t)$ of the Bessel function now
872 appears as $1/T_{el}$ multiplied by the time integral of $F(t)$,
873 which, as defined in Appendix A, is just the time-dependent
874 FC factor $F(t)$ reflecting the overlap between vibrational
875 wave functions in ground and excited electronic states. Al-
876 though this result is analytic and appealingly simple and al-
877 though not readily seen from the derivation given by Magee
878 and Funabashi,⁴¹ the final approximation leading to Eq. (A8)
879 of Appendix A is somewhat drastic in that it demands that,
880 for fixed time, the FC factors between monomer n and both
881 neighbors $n \pm 1$ are identical.

882 We consider three special cases. The first two provide
883 just the known analytic solutions from Sec. IV A. First we
884 assume the CES approximation that the excited electronic
885 state vibrational wave function is of the form,

$$886 \quad |\Sigma_e^n(t)\rangle = |\chi_n(t)\rangle \prod_{m \neq n} |\xi_m^0\rangle \quad (48)$$

887 and, see Appendix A,

$$888 \quad F(t) = \langle \Sigma_e^n(t) | \Sigma_e^{n \pm 1}(t) \rangle = \langle \chi_n(t) | \xi_n^0 \rangle \langle \xi_{n \pm 1}^0 | \chi_{n \pm 1}(t) \rangle. \quad (49)$$

889 The wavepacket $|\chi_m(t)\rangle$ is that produced upon vertical elec-
890 tronic excitation of monomer m from the ground vibrational
891 state $|\xi_m^0\rangle$. The initial condition is $|\chi_n(0)\rangle = |\xi_n^0\rangle$ and then the
892 wavepacket develops in time in the excited-state potential
893 curve. In the first case, the extreme strong-coupling limit, the
894 excitation is passed on to the neighboring monomer before
895 there is any time for the wavepacket to change. Then $F(t)$
896 = 1 and $\gamma(t) = (2V/\hbar)t$, exactly the result of Eq. (38). In the
897 second case we consider only a single vibrational eigenstate
898 α in the upper potential curve. Then $F(t) = |f_0^\alpha|^2$ and the prob-
899 ability for coherent excitation transfer is

$$900 \quad P_{n0}^\alpha(t) = J_n^2 \left(\frac{2V}{\hbar} |f_0^\alpha|^2 t \right). \quad (50)$$

901 The total probability, starting from an initial distribution p_α
902 = $|f_0^\alpha|^2$ is given by

$$903 \quad P_{n0}(t) = \sum_\alpha |f_0^\alpha|^2 J_n^2 \left(\frac{2V}{\hbar} |f_0^\alpha|^2 t \right), \quad (51)$$

904 which is identical to Bierman's result of Eq. (42), the ex-
905 tremely weak-coupling case.

The third and most important case is where we consider 906
a continuous monomer absorption spectrum, corresponding 907
to coupling to EM vibrations. It is clear that the absence of 908
discrete vibrational structure indicates that the wavepacket 909
 $\chi(t)$ does not oscillate back and forth in the upper BO poten- 910
tial curve, as is necessary for the formation of eigenstates. 911
Rather the continuum in energy space corresponds to a 912
wavepacket which moves out continually in space and does 913
not return. This behavior mimics the continuous broadening 914
of the vibrational eigenstates due to coupling to the continu- 915
ous spectrum of EM vibrations. The simplest way to model 916
this behavior is to take, not a harmonic potential but a simple 917
linear potential in the upper state [see Fig. 1(b)]. The mono- 918
mer absorption spectrum is proportional to $-\text{Im}\langle g(E) \rangle$. For 919
example, from Eq. (28), we have 920

$$\text{Im}\langle g(E) \rangle = \pi \sum_\alpha |f_0^\alpha|^2 \delta(E - E_\alpha), \quad (52) \quad 921$$

showing absorption in discrete spectral lines. By contrast, in 922
the continuous case for a linear potential, from Eq. (B6) of 923
Appendix B one has, in terms of the dimensionless energy ϵ 924
(defined in Appendix B), 925

$$\text{Im}\langle g(\epsilon) \rangle \propto e^{-\epsilon^2}, \quad (53) \quad 926$$

which is a continuous single Gaussian absorption spectrum. 927
Clearly, more complicated vibronic absorption spectra can be 928
fitted by a sum of such Gaussians. From Eqs. (48) and (49), 929
one sees that, taken independent of n , the function $F(t)$ is 930
given by 931

$$F(t) = |\langle \chi(t) | \xi^0 \rangle|^2 = |\langle \xi^0 | g(t) | \xi^0 \rangle|^2 \equiv |\langle g(t) \rangle|^2 \quad (54) \quad 932$$

so that, from Eq. (47) and Eq. (B7) of Appendix B, we have 933

$$\begin{aligned} \gamma(t) &= \frac{2V}{\hbar} \int_0^t \exp \left[- \left(\frac{t'}{T_{\text{vib}}} \right)^2 \right] dt' \\ &= \frac{2V}{\hbar} \frac{\sqrt{\pi}}{2} T_{\text{vib}} \text{erf} \left[\frac{t}{T_{\text{vib}}} \right], \end{aligned} \quad (55) \quad 934 \quad 935$$

where $T_{\text{vib}} = \hbar / \sigma_G$ can be thought of as a characteristic vi- 936
bronic coupling time since σ_G is the width of the Gaussian 937
vibronic absorption spectrum. This general result satisfies 938
two limits. The first is the limit $t \rightarrow 0$ when $\text{erf}(t/T_{\text{vib}})$ 939
 $\rightarrow (2/\sqrt{\pi})(t/T_{\text{vib}})$ so that $\gamma = (2V/\hbar)t$ and we recover the 940
strong-coupling case, where the initial wavepacket has no 941
time to move before it is handed on. The second limit is 942
 $(t/T_{\text{vib}}) \rightarrow \infty$ when $\text{erf}(t/T_{\text{vib}}) \rightarrow 1$ and we have 943

$$\gamma(t) = \frac{2V}{\hbar} \frac{\sqrt{\pi}}{2} T_{\text{vib}} \approx \frac{T_{\text{vib}}}{T_{\text{el}}} = \frac{2V}{\sigma_G}. \quad (56) \quad 944$$

Hence, this theory predicts that at large times a fixed prob- 945
ability distribution $P_n(\gamma)$ emerges, i.e., the exciton becomes 946
trapped. Clearly the realization of this long-time limit for a 947
single monomer requires that the excitation is not transferred 948
to a neighbor within this time, i.e., that $T_{\text{vib}}/T_{\text{el}} \leq 1$. That is, 949
as the numerical solutions show, only in weak and interme- 950
diate coupling, is there trapping of the exciton. Note also 951
that, for a continuous spectrum, the extremely weak-coupling 952

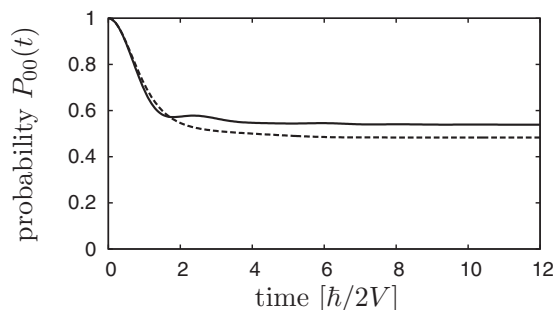


FIG. 14. The probability $P_{00}(t)$ that excitation resides on monomer zero as a function of time in units of T_{el} . The parameters are $2V=1$, $\sigma_G=0.38$, and $X=0.61$ [corresponding to Fig. 13(o) and the broadest spectrum in Fig. 12]. Solid line: CES approximation. Dashed line: Magee–Funabashi approximation.

(2) In general, one has

$$\frac{d\bar{n}}{dt} = (V/\hbar) \sum_{\alpha} \sum_{\beta} |f_0^{\alpha}|^2 |f_0^{\beta}|^2 \exp[-i(E_{\alpha} - E_{\beta})t/\hbar]. \quad (61)$$

This illustrates that the reduction in velocity encountered when the single electronic transition is split into many vibronic (but still discrete) transitions is due to a dephasing arising from the many different frequencies in the double sum in this equation for the velocity. The number of vibronic levels involved in the sum increases with increasing vibronic coupling (increasing X), which explains the strong reduction of propagation velocity with increasing X shown in Fig. 5

(3) In the continuum limit $X \rightarrow \infty$ and $\omega \rightarrow 0$ with σ constant, the FC Poissonian distribution of Eq. (1) becomes a Gaussian distribution in energy, corresponding to the linear potential result of Eq. (53). Correspondingly, the Fourier series [Eq. (60)] becomes the Fourier transform of a continuous Gaussian distribution leading to the time-dependent Gaussian $\langle g(\tau) \rangle = \exp(-\tau^2/2)$ of Eq. (B7), where τ is the dimensionless time $\tau = t/T_{vib}$. This correspondence justifies our numerical procedure of treating the continuum as a very large number of densely packed discrete transitions. One can also interpret the trapping phenomenon arising from a continuous spectrum as due to the interference of infinitely many phase factors appearing in Eq. (61) which damps out the propagation at large τ , i.e., large times $t \gg T_{vib}$.

V. CONCLUSIONS

We have examined the transfer of electronic excitation (EET) on a chain of molecules which interact via electronic coupling and which have a ground and one excited electronic level. The electronic levels are considered to couple both to internal vibrational modes of the monomer (IM) and EMs of the surroundings. The IM are specified as giving a single dominant vibrational progression, as seen, for example, in the monomer spectrum of many dye molecules forming large aggregates. The EMs are not included specifically but are assumed to give rise to a continuous vibronic absorption spectrum, again typical of many organic molecules in solution.

The probability $P_n(t)$ that, beginning with electronic excitation localized on a single monomer, the excitation has propagated a distance of n monomers can be expressed in terms of matrix elements of the time propagator or time-dependent Green's operator $G(t)$. Initially, for small aggregates and a single discrete IM vibration, we have performed the time propagation exactly numerically. For strong coupling ($SP \rightarrow \infty$), which corresponds to the limit of vanishing vibronic coupling ($X \rightarrow 0$), $P_n(t)$ shows an oscillatory behavior. The effect of increasing vibronic coupling is to damp the amplitude of the oscillations and to lengthen their period. The net result is an effective slowing or inhibition of the migration of the excitation away from the initial site. Nevertheless, in the course of time the excitation propagates over

case of Bierman, which requires the condition $2V \leq \hbar\omega$, will not occur since effectively $\omega \rightarrow 0$.

To illustrate that the analytic approximation explains the trapping we have calculated $P_{00}(t) = |J_0(\gamma(t))|^2$ using Eq. (49) and Eq. (B8) of Appendix B. The result shown in Fig. 14 is compared with the result of the CES approximation numerical calculation for the case shown in Fig. 13(o). Clearly one sees that the analytic Magee–Funabashi approximation gives a good description of the rate of approach to a time-independent probability, i.e., trapping of the excitation.

Finally we discuss the mean velocity of propagation of the electronic excitation. The mean square propagation distance is given by

$$\overline{n^2(t)} = \sum_{n=0}^{\infty} n^2 |J_n(\gamma(t))|^2 = \gamma^2(t)/4. \quad (57)$$

Hence,

$$\bar{n}(t) = \gamma(t)/2 = (V/\hbar) \int_0^t |\langle g(t') \rangle|^2 dt' \quad (58)$$

and the time-dependent mean velocity is

$$\frac{d\bar{n}}{dt} = (V/\hbar) |\langle g(t) \rangle|^2. \quad (59)$$

For a discrete monomer spectrum $\langle g(t) \rangle$ is calculated easily by Fourier transform of $\langle g(E) \rangle$ of Eq. (28) to give

$$\langle g(t) \rangle = \sum_{\alpha} |f_0^{\alpha}|^2 \exp(-iE_{\alpha}t/\hbar). \quad (60)$$

Three points are noteworthy here.

(1) If the distribution with width $\sigma = \sqrt{X\hbar\omega}$ is small with respect to $2V$, we can replace E_{α} by the average energy \bar{E} . This leads to $\langle g(t) \rangle = \exp(-i\bar{E}t/\hbar)$ and to the strong-coupling pure electronic result $d\bar{n}/dt = V/\hbar$, as expected.

1034 the complete aggregate. The CES approximation, which re-
 1035 stricts the occupation to the lowest vibrational state of the
 1036 ground electronic state, has been shown to give good overall
 1037 agreement with the exact results. This approximation has the
 1038 advantage that extremely long aggregates (of the order of
 1039 100 monomers) can be handled numerically and, in certain
 1040 limits, analytical solutions for matrix elements of $G(t)$ can be
 1041 obtained. Taking advantage of this simplification and with a
 1042 combination of numerical and analytical solutions we have
 1043 established the following characteristics of the propagation
 1044 of vibronic excitation.

- 1045 (1) In the pure electronic case, excitation is an oscillatory
 1046 function of time and propagates with constant mean
 1047 velocity from the site of initial excitation. This charac-
 1048 teristic is largely retained when vibronic coupling is
 1049 included but $SP \gg 1$, i.e., strong coupling.
- 1050 (2) In the case of a discrete spectrum (single IM vibration),
 1051 for intermediate coupling the regular pattern of propa-
 1052 gation is destroyed, probability becomes smeared out in
 1053 an irregular fashion, and there is a reduction in the
 1054 mean velocity of propagation.
- 1055 (3) In the case of a discrete spectrum, for weak coupling, a
 1056 quasiregular pattern of propagation is restored (in
 1057 agreement with the analytical result of Bierman) but at
 1058 a considerably lower velocity than that predicted by the
 1059 purely electronic case.
- 1060 (4) The above features can all be explained by approximate
 1061 analytic solutions in which $P_n(t)$ is expressed in terms
 1062 of Bessel functions. In particular, the constant velocity
 1063 limits in strong and weak couplings are explained. The
 1064 inhibition and irregularity of propagation in the inter-
 1065 mediate coupling case is shown to be due to a dephas-
 1066 ing arising from the many different pathways of trans-
 1067 fer between adjacent monomers when many vibronic
 1068 levels participate.
- 1069 (5) When coupling to EM is included by a transition to a
 1070 continuous spectrum, a new phenomenon appears in the
 1071 numerical solutions in that, in the course of time, the
 1072 propagation velocity goes to zero, i.e., the exciton be-
 1073 comes trapped with a fixed distribution P_n independent
 1074 of time. This trapping has also been explained analyti-
 1075 cally by a simple model of an upper linear BO potential
 1076 such that the vibrational wavepacket moves out from
 1077 the FC overlap region with the ground BO potential
 1078 and does not return. Then the trapping time is just the
 1079 time taken for the overlap to go to zero, which turns out
 1080 to be on the order of \hbar/σ , where σ is the width of the
 1081 continuous monomer vibronic spectrum.

1082 Our aim in this study has been not to give a detailed
 1083 numerical simulation of any particular EET process but to
 1084 establish the main characteristics of EET coupled to vibra-
 1085 tions and to isolate the physical parameters governing these
 1086 characteristics. To simplify the study of propagation, we
 1087 have assumed that electronic excitation is localized initially
 1088 on a single monomer. However, in a real experiment it is
 1089 probable that light absorption leads to simultaneous finite
 1090 probability of many monomers, i.e., an initially delocalized
 1091 exciton. Hence the rather small transfer distances that are

1092 predicted before trapping when the spectrum is broad and
 1093 continuous may not indicate that excitation is localized over
 1094 such distances. 1094

1095 It must also be pointed out which physical processes are
 1096 not taken into account here. In this respect the major omis-
 1097 sion is that of coupling between the vibrational degrees of
 1098 freedom, whether IM or EM, themselves. This will lead to
 1099 dissipation of the energy of excitation and accumulation of
 1100 probability in the lowest vibrational states of each BO poten-
 1101 tial. Similarly, finite temperature will alter the occupation of
 1102 vibronic levels. In the case of the trapping of excitation pre-
 1103 dicted when the vibronic spectrum is continuous, we have
 1104 not considered the further fate of the wavepacket after leav-
 1105 ing the FC region. Clearly, coupling to other processes, e.g.,
 1106 dissociation of the exciton, presence of acceptor molecules,
 1107 and radiative decay, will disturb the establishment of a time-
 1108 independent probability distribution of the electronic excita-
 1109 tion. However, the model can be extended, albeit numeri-
 1110 cally, to include such couplings. Also the CES approximation
 1111 used ignores part of the vibrational structure of the ground
 1112 electronic state, which may also play a role in the transfer
 1113 dynamics. Finally, to expose more clearly the main physical
 1114 mechanisms operating, we have restricted discussion to the
 1115 simplest geometry, that of a linear or circular chain of mono-
 1116 mers. In applications the precise geometry of the three-
 1117 dimensional aggregate must be taken into account, usually
 1118 giving a larger number of nearest or near neighbors between
 1119 which EET can occur. In some cases, e.g., Refs. 7 and 45, an
 1120 effective linear geometry appears a good approximation;
 1121 however, in others, e.g., Refs. 46–49, the aggregate is two or
 1122 three dimensional. 1122

1123 Since this is a model study, the main results are not
 1124 restricted to the particular case of an aggregate of electroni-
 1125 cally coupled large organic molecules. In particular, the ana-
 1126 lytical approximations should be applicable to other quantum
 1127 aggregates modeled by two-level monomers with superim-
 1128 posed vibrational structure, such as are listed in Sec. I. 1128

ACKNOWLEDGMENTS 1129

1130 Financial support of this work by the DFG under Project
 1131 No. Br 728/11 is gratefully acknowledged. 1131

APPENDIX A: 1132

1133AQ: We differentiate Eq. (3) of the text and obtain (for times
 1134 #9 $t > 0$) 1134

$$\frac{\partial}{\partial t} G(t) = -\frac{i}{\hbar} H G(t). \quad (\text{A1}) \quad 1135$$

1136 Taking electronic matrix elements and inserting a unit opera-
 1137 tor between H and $G(t)$, one gets 1137

$$\begin{aligned}
1138 \quad \frac{\partial G_{nm}(t)}{\partial t} &= -(i\hbar) \sum_{n'} H_{nn'} G_{n'm}(t) \\
&= -(i\hbar) \sum_{n'} V_{nn'} G_{n'm}(t) - (i\hbar) K_{\text{mon}}^n G_{nm}(t), \\
1139 & \tag{A2}
\end{aligned}$$

1140 where K_{mon}^n is a sum of single monomer BO vibrational
1141 Hamiltonians with monomer n excited electronically (ϵ_{el} is
1142 taken as the arbitrary zero of energy). This equation remains
1143 an operator equation in the space of vibrational coordinates.
1144 To remove the last term in Eq. (A2) we define a time-
1145 dependent vibrational state $|\Sigma_e^n(t)\rangle$ of the polymer by the
1146 equation

$$1147 \quad \left(K_{\text{mon}}^n - i\hbar \frac{\partial}{\partial t} \right) |\Sigma_e^n(t)\rangle = 0. \tag{A3}$$

1148 Then, we have

$$\begin{aligned}
1149 \quad \frac{d}{dt} \langle \Sigma_e^n(t) | G_{nm}(t) | \Sigma_g \rangle &= \langle \Sigma_e^n | \frac{\partial G_{nm}(t)}{\partial t} | \Sigma_g \rangle \\
&+ \left\langle \frac{\partial \Sigma_e^n}{\partial t} | G_{nm}(t) | \Sigma_g \right\rangle. \\
1150 & \tag{A4}
\end{aligned}$$

1151 Taking the appropriate matrix element of Eq. (A2), we obtain

$$\begin{aligned}
\frac{d}{dt} \langle \Sigma_e^n(t) | G_{nm}(t) | \Sigma_g \rangle &= -(i\hbar) \sum_{n'} V_{nn'} \langle \Sigma_e^n(t) | G_{n'm}(t) | \Sigma_g \rangle. \\
1152 & \tag{A5}
\end{aligned}$$

1153 Since the coupling matrix element on the right hand side of
1154 the above equation involves both n and n' it is not possible
1155 to proceed further without approximation. Since the operator
1156 $G_{n'm}$ places monomer n' in the excited electronic state, one
1157 introduces, as an approximation to the unit operator, the pro-
1158 jector $|\Sigma_e^{n'}(t)\rangle \langle \Sigma_e^{n'}(t)|$ into the coupling term, i.e.,

$$\begin{aligned}
1159 \quad \frac{d}{dt} \langle \Sigma_e^n(t) | G_{nm}(t) | \Sigma_g \rangle &= -(i\hbar) \sum_{n'} V_{nn'} \langle \Sigma_e^n(t) | \Sigma_e^{n'}(t) \rangle \\
&\times \langle \Sigma_e^{n'}(t) | G_{n'm}(t) | \Sigma_g \rangle. \\
1160 & \tag{A6}
\end{aligned}$$

1161 Then, restricting to nearest-neighbor coupling, arbitrarily fix-
1162 ing $m=0$ and taking $V_{n,n-1}=V_{n,n+1}=V$ for identical mono-
1163 mers, one has the set of equations,

$$\begin{aligned}
1164 \quad \frac{d}{dt} b_n(t) &= -(i\hbar)V [\langle \Sigma_e^n(t) | \Sigma_e^{n-1}(t) \rangle b_{n-1}(t) \\
&+ \langle \Sigma_e^n(t) | \Sigma_e^{n+1}(t) \rangle b_{n+1}(t)], \\
1165 & \tag{A7}
\end{aligned}$$

1166 where we have set $b_m = \langle \Sigma_e^m(t) | G_{m0}(t) | \Sigma_g \rangle$. The final approxi-
1167 mation is to take $\langle \Sigma_e^n(t) | \Sigma_e^{n+1}(t) \rangle = F(t)$ to be independent of
1168 n . This approximation leads to the simple set of coupled
1169 equations,

$$1170 \quad \frac{d}{dt} b_n(t) = -(i\hbar)VF(t)[b_{n-1}(t) + b_{n+1}(t)]. \tag{A8}$$

1171 As Magee and Funabashi⁴¹ showed, these coupled equations
1172 have the solution,

$$b_n(t) = \exp(-in\pi/2)J_n(\gamma(t)), \tag{A9} \quad 1173$$

where 1174

$$\gamma(t) = (2V/\hbar) \int_0^t F(t') dt'. \tag{A10} \quad 1175$$

APPENDIX B: 1176

The monomer energy-dependent Green's function with
the upper BO potential approximated by a linear form with
slope a [see Fig. 1(b)] is given by the equation 1178

$$\left(\frac{\hbar^2}{2} \frac{\partial^2}{\partial Q^2} + E - \epsilon_{\text{el}} + aQ + \epsilon_0 \right) g(Q, Q', E) = \delta(Q, Q') \tag{B1} \quad 1180$$

The ground-state vibrational potential is assumed harmonic,
with rest energy $\epsilon_0 = \hbar\omega/2$ and with ground eigenfunction, 1182

$$\xi_0 = (b^{1/2}/\pi^{1/4}) \exp(-b^2 Q^2/2), \tag{B2} \quad 1183$$

where $b^2 = 2\omega/\hbar$. Transforming to the dimensionless variable
 $x = bQ$ gives a monomer Green's function defined by 1185

$$\kappa \frac{\partial^2 g}{\partial x^2} + (\epsilon + \kappa + x)g(x, x') = (b^2/a) \delta(x - x'), \tag{B3} \quad 1186$$

where we define the dimensionless quantities κ
 $= \hbar\omega/(2a/b)$ and $\epsilon = (E - \epsilon_{\text{el}})/(a/b)$. In Ref. 50 it is shown
that an integral representation of $g(x, x')$ can be derived from
which an integral representation of the ground-state expecta-
tion value $\langle g(\epsilon) \rangle$ can be calculated, i.e., 1191

$$\begin{aligned}
\langle g(\epsilon) \rangle &= \int_0^\infty \xi_0(x) g(x, x', \epsilon) \xi_0(x') dx dx' \\
&= -i(a/b) \int_0^\infty \frac{\exp(-ikx^3/12 - x^2/4)}{(ikx+1)^{1/2}} e^{i\epsilon x} dx. \\
1192 & \tag{B4} \quad 1193
\end{aligned}$$

From this form, the Fourier transform to time space is easily
performed to give $\langle g(\tau) \rangle$ and 1195

$$|\langle g(\tau) \rangle|^2 = \frac{\exp(-\tau^2)}{(\kappa^2 \tau^2 + 1)^{1/2}}, \tag{B5} \quad 1196$$

where τ is the dimensionless time $\tau = t/T_{\text{vib}}$. Since κ is usu-
ally much less than unity, the approximation $\kappa=0$, which
amounts to neglecting the kinetic energy near to the turning
point, is often a good approximation. Then Eq. (B4) can be
evaluated in closed form to give 1201

$$\langle g(\epsilon) \rangle = \frac{b}{a} e^{-\epsilon^2} (2 \operatorname{erf}(-i\epsilon) - i\sqrt{\pi}), \tag{B6} \quad 1202$$

whose imaginary part gives a continuous Gaussian absorp-
tion spectrum (see also Refs. 30 and 31). Correspondingly,
for $\kappa=0$, Eq. (B5) reduces to the simple form 1205

$$|\langle g(\tau) \rangle|^2 = \exp(-\tau^2), \tag{B7} \quad 1206$$

showing explicitly that the outgoing motion of the excited-
state vibrational wavepacket leads to a decay in time of the
effective FC factor for transfer between electronic ground
state and electronic excited state. In the dimensionless time
 $\tau = t/T_{\text{vib}}$, the scale time T_{vib} is given by $T_{\text{vib}} = \sqrt{2\hbar}/(a/b)$ 1211

1212 $=\hbar/\sigma_G$ since $(a/\sqrt{2}b)$ is the width σ_G , in dimensions of en-
1213 ergy, of the monomer continuous Gaussian absorption spec-
1214 trum obtained from Eq. (B6). Hence T_{vib} can be viewed as a
1215 typical time for the onset of vibronic coupling.

1216 In the case of Fig. 12 where the absorption spectrum is
1217 fitted by a sum of Gaussians, Eq. (B7) must be suitably
1218 modified. In this case the spectrum can be viewed as the
1219 convolution of a stick spectrum with a set of Gaussians cen-
1220 tered at the sticks. Hence, the Fourier transform to time space
1221 consists of a product of the separate Fourier transforms of the
1222 Gaussian and the stick spectrum. Then it is easy to show that
1223 Eq. (B7) is generalized to

$$\langle |g(\tau)|^2 \rangle = \exp(-\tau^2) \left| \sum_{\alpha} |f_0^{\alpha}|^2 \exp(i\epsilon_{\alpha}\tau) \right|^2, \quad (\text{B8})$$

1225 where $\epsilon_{\alpha} = E_{\alpha} / \sigma_G = \alpha(\hbar\omega) / \sigma_G$.

- 1226** ¹A. Davydov, *Theory of Molecular Excitons* (McGraw-Hill, New York,
1227 1962).
1228 ²H. Haken and P. Reineker, *Z. Phys.* **249**, 253 (1971).
1229 ³H. Haken and G. Strobl, *Z. Phys.* **262**, 135 (1973).
1230 ⁴P. O. J. Scherer, E. W. Knapp, and S. F. Fischer, *Chem. Phys. Lett.* **106**,
1231 191 (1984).
1232 ⁵C. Supritz, V. Gounaris, and P. Reineker, *J. Lumin.* **128**, 877 (2008).
1233 ⁶*J-Aggregates*, edited by T. Kobayashi (World Scientific, Singapore,
1234 1996).
AQ:1235 ⁷H. van Amerongen, L. Valkunas, and R. van Grondelle, *Photosynthetic*
#101236 *Excitons* (World Scientific, Singapore, 2000).
1237 ⁸T. Brixner, J. Stenger, H. M. Vaswani, M. Cho, R. E. Blankenship, and G.
1238 R. Fleming, *Nature (London)* **434**, 625 (2005).
1239 ⁹O. Kühn and V. Sundström, *J. Chem. Phys.* **107**, 4154 (1997).
1240 ¹⁰T. Renger and V. May, *J. Phys. Chem. A* **102**, 4381 (1998).
1241 ¹¹P. Rebentrost, M. Mohseni, I. Kassal, S. Lloyd, and A. Aspuru-Guzik,
1242 *New J. Phys.* **11**, 033003 (2009).
1243 ¹²F. Robicheaux, J. V. Hernández, T. Topçu, and L. D. Noordam, *Phys.*
1244 *Rev. A* **70**, 042703 (2004).
1245 ¹³C. Ates, A. Eisfeld, and J. M. Rost, *New J. Phys.* **10**, 045030 (2008).
1246 ¹⁴O. Müllen, A. Blumen, T. Amthor, C. Giese, M. Reetz-Lamour, and M.
1247 Weidemüller, *Phys. Rev. Lett.* **99**, 090601 (2007).
1248 ¹⁵G. D. Scholes and G. Rumbles, *Nature Mater.* **5**, 683 (2006).
1249 ¹⁶G. P. Wiederrecht, G. A. Wurtz, and J. Hranisavljevic, *Nano Lett.* **4**,
1250 2121 (2004).
1251 ¹⁷P. Walczak, A. Eisfeld, and J. S. Briggs, *J. Chem. Phys.* **128**, 044505
1252 (2008).
1253 ¹⁸M. Wewer and F. Stienkemeier, *J. Chem. Phys.* **120**, 1239 (2004).

- ¹⁹M. Schreiber and Y. Toyozawa, *J. Phys. Soc. Jpn.* **51**, 1528 (1982). **1254**
²⁰H. Fidder, J. Knoester, and D. A. Wiersma, *J. Chem. Phys.* **95**, 7880 **1255**
(1991). **1256**
²¹C. Didraga and J. Knoester, *J. Chem. Phys.* **121**, 10687 (2004). **1257**
²²P. Hefman, U. Kleinekathöfer, I. Barvik, and M. Schreiber, *Chem. Phys.* **1258**
275, 1 (2002). **1259**
²³E. W. Knapp, *Chem. Phys.* **85**, 73 (1984). **1260**
²⁴V. A. Malyshev, *J. Lumin.* **55**, 225 (1993). **1261**
²⁵A. V. Malyshev, V. A. Malyshev, and F. Dominguez-Adame, *J. Phys.* **1262**
Chem. B **107**, 4418 (2003). **1263**
²⁶V. A. Malyshev, A. Rodriguez, and F. Dominguez-Adame, *Phys. Rev. B* **1264**
60, 14140 (1999). **1265**
²⁷M. Bednarz, V. A. Malyshev, and J. Knoester, *Phys. Rev. Lett.* **91**, **1266**
217401 (2003). **1267**
²⁸M. Bednarz, V. A. Malyshev, and J. Knoester, *J. Chem. Phys.* **120**, 3827 **1268**
(2004). **1269**
²⁹E. S. Medvedev and V. I. Osherov, *Radiationless Transitions in Poly-*
atomic Molecules, Springer Series in Chemical Physics Vol. 57 (Springer-
Verlag, Berlin, 1995). **1270**
³⁰R. Schinke, *Photodissociation Dynamics* (Cambridge University Press, **1273**
Cambridge, 1995). **1274**
³¹S. Koller, J. Seibt, P. Marquetand, and V. Engel, *Chem. Phys. Lett.* **433**, **1275**
199 (2006). **1276**
³²J. S. Briggs and A. Herzenberg, *Mol. Phys.* **21**, 865 (1971). **1277**
³³A. Eisfeld and J. S. Briggs, *Chem. Phys.* **281**, 61 (2002). **1278**
³⁴A. Eisfeld and J. S. Briggs, *Phys. Rev. Lett.* **96**, 113003 (2006). **1279**
³⁵A. Eisfeld and J. S. Briggs, *Chem. Phys.* **324**, 376 (2006). **1280**
³⁶A. Eisfeld, R. Kniprath, and J. Briggs, *J. Chem. Phys.* **126**, 104904 **1281**
(2007). **1282**
³⁷A. Eisfeld and J. S. Briggs, *Chem. Phys. Lett.* **446**, 354 (2007). **1283**
³⁸W. T. Simpson and D. L. Peterson, *J. Chem. Phys.* **26**, 588 (1957). **1284**
³⁹R. E. Merrifield, *J. Chem. Phys.* **28**, 647 (1958). **1285**
⁴⁰A. Bierman, *J. Chem. Phys.* **46**, 2124 (1967). **1286**
⁴¹J. L. Magee and K. Funabashi, *J. Chem. Phys.* **34**, 1715 (1961). **1287**
⁴²J. Roden, A. Eisfeld, and J. S. Briggs, *Chem. Phys.* **352**, 258 (2008). **1288**
⁴³B. Koppinsky, J. K. Hallermeier, and W. Kaiser, *Chem. Phys. Lett.* **83**, **1289**
498 (1981). **1290**
⁴⁴A. Eisfeld, L. Braun, W. T. Strunz, J. S. Briggs, J. Beck, and V. Engel, *J.*
Chem. Phys. **122**, 134103 (2005). **1291**
⁴⁵M. Hoffmann, K. Schmidt, T. Fritz, T. Hasche, V. M. Agranovich, and K. **1293**
Leo, *Chem. Phys.* **258**, 73 (2000). **1294**
⁴⁶S. Kirstein and S. Dähne, *Int. J. Photoenergy* **■**, 20363 (2006). **1295AQ:**
⁴⁷D. Möbius and H. Kuhn, *J. Appl. Phys.* **64**, 5138 (1988). **1296#11**
⁴⁸S. S. Lampoura, C. Spitz, S. Dähne, J. Knoester, and K. Duppen, *J. Phys.* **1297**
Chem. B **106**, 3103 (2002). **1298**
⁴⁹V. I. Prokhorenko, D. B. Steensgaard, and A. R. Holzwarth, *Biophys. J.* **1299**
85, 3173 (2003). **1300**
⁵⁰J. S. Briggs, Ph.D. thesis, Victoria University of Manchester, 1968. **1301**

AUTHOR QUERIES — 043928JCP

- #1 Au: Please check insertion of postal code in the first affiliation. Also, please supply city and postal code for the second affiliation.
- #2 Au: Please check insertion of “Appendixes A and B” in place of “appendix” and supply Appendix Titles.
- #3 Au: Please check edit in the sentence “We have applied extensively the approach...” to see if meaning is preserved.
- #4 Au: Please check edit in the sentence “The simplest way to study EET is...”
- #5 Au: Please check deletion of asterisk in Eq. (17).
- #6 Au: Please check edit in the sentence “The CES results for...” to see if meaning is preserved.
- #7 Au: Please check changes in Eq. (37).
- #8 Au: Please check edit in the sentence “The monomer number...” to see if meaning is preserved.
- #9 Au: Please supply title for Appendixes A and B.
- #10 Au: Please check insertion of publisher’s location in Refs. 1, 6, 29, and 30.
- #11 Au: Please supply volume number in Ref. 46.